



CERTAIN NONLINEAR AND UNCERTAIN SYSTEMS: SOME ASPECTS OF OBSERVER BASED SLIDING MODE CONTROL

¹Sharoon Aziz Choudhary, ²Dr. Deena Lodwal Yadav

¹Student, ²Assistant Professor

¹Electrical Engineering,

¹UIT RGPV, Bhopal, India

ABSTRACT: Observer is used to estimate the state of system which are difficult to measure are often unpredictable due to some limitation or constraint under which system is subjected. Conventional observer is less robust against matched and mismatched uncertainty. While sliding mode observer is more robust as compared to conventional observer. But sliding mode observer needs filter to estimate the states of system which leads to complexity from design point of view. Higher order sliding mode observer removes all problems and provide robust response against matching and mismatching disturbances are presented in next paper. The most recent research in control theory indicates that a system is referred to as a state observer when it estimates the internal state of a particular actual system by measuring its inputs and outputs. With the assistance of computers, it is frequently implemented, and it is the basis for many useful applications. Many control theory problems can be solved by knowing the state of the system, such as stabilizing a system with state feedback. Most of the time, it is not possible to determine a system's state directly by observing its physical condition. As a result, it is possible to observe indirect repercussions of the system's current internal state through its outputs. It is possible to monitor the rates and speeds at which vehicles enter and exit the tunnel directly, but only educated guesses can be made about the conditions inside. Please consider this simple illustration. The state observer can rebuild a system's state based on measurements of its output if the system is observable. The system must be observable in order for this to be possible.

Keywords: Observer Based Sliding Mode Control, Nonlinear Systems, Uncertain Systems, Mathematical Modeling, Observer Design, Sliding Mode Control, Stability Analysis, Integration.

1. INTRODUCTION

The challenge of load frequency control, sometimes referred to as LFC, is faced by many power networks. The LFC is aimed at balancing load demand parameters like frequency variation and tie lines with degeneration. Many control zones that are distinguished by a multi-area power system approach zero in terms of power deviation [33–36]. In this work, the random load perturbation was modelled as Gaussian white noise. With the aid of the delta correlated autocorrelation function (37), white noise can be characterized. A variety of reasons, including the wide range of applications, are driving research into the control of uncertain nonlinear systems. In [38-41]. As energy is exchanged over link lines in a power system serving multiple areas, frequency management becomes more difficult. Since it only requires the state information of the local region to reduce frequency difference, a decentralised LFC technique is more useful for everyday situations than a centralised one.

As a result of various uncertainties, various control strategies have been put forth to address frequent issues. In order to address load frequency control (LFC) issues in connected power systems, both traditional and novel approaches have been used [42–48]. A linearized model based on fixed PI parameters is the basis for designing loading frequency controllers. The first step toward solving LF concerns was research on PI control. It is typical for traditional PI controllers

to have permanent and constant structures, and to configure their settings according to operational conditions [43][44]. LFC typically uses an integrated surface. Having a large integral gain can negatively impact the performance of a system, causing oscillations and instability. By keeping the gain low, this can be avoided. Due to this, the integral gain must be calibrated to achieve the desired level of transient recovery while maintaining a low level of overshoot. The processes that can be used to modify the gain of the integrated controller have been outlined in [36] and [37]. PI control strategy, on the other hand, produces larger transient responses as well as a much longer stabilization period. As well, the PI control algorithm does not produce the required response until the system is very close to the point where it is intended to operate.

As a result, they cannot function properly in the presence of numerous load disturbance fluctuations and parameter uncertainties associated with multi-area power systems. In order to optimise PI controller parameters in the presence of parameter uncertainty and load disturbances, resilient and clever solutions have been put forth. The effectiveness of the system as a whole has increased as a result of these techniques. 48 and 50. The appearance of terminating transmissions, the stochastic process, the jitter, and packet loss are common characteristics of signal transmission in network communications, especially shared communications, which can degrade performance. These problems are more frequent in shared communications, in particular. Power system instability is present [51]. SMC [52] asserts that a number of application systems, including uncertain systems, are becoming more and more common. A standard LFC controller can only function in close proximity to the nominal point and is built with fixed settings [44]. According to M. Yang, the only time that an SMLFC demonstrates the best improved response is when a compatible system is also present, as well as unmatched uncertainties, stepwise load disruption, system non-linearity, and stochastic perturbations [28].

2. Multi-area power system model with stochastic perturbation

Despite the dynamic and nonlinear nature of the power system model, the linearized model can still be used to control the charge frequency. During normal operation, load variations are only modest [28]. A power system serving multiple locations requires, in addition to additional control actions in the extra control operations in the secondary loop after the primary speed control loop. Therefore, despite being a complex non-linear system, the power network can be conceptualised as linearized for the purposes of the study. The real plant will always differ from its mathematical model when it comes to formulating real control problems. The reason for this is that there are many different types of uncertain load disturbances, both internal and external. Thus, the dynamic equations of the linked power system model require the following adjustments in order to account for this:

On the probability space (F, P) , include the following uncertain stochastic perturbation:

$$dx_i(t) = \left[\begin{array}{l} (A_i + \tilde{A}_i(t))x_i(t) + B_i u_i(t) + \\ D_i w_i(t) + \sum_{\substack{j \in N \\ j \neq i}} E_{ij} x_j(t) + F_i \Delta P_{d_i}(t) \end{array} \right] dt + H_i f_i(x(t), y(t)) d\varpi_i(t) \quad (4.1)$$

$$y_i(t) = C_i x_i(t) \quad (4.2)$$

where $x_i(t) \in R^{n_i}$ denotes the state vector, $u_i(t) \in R^{m_i}$ is the control input, $x_j(t) \in R^{n_j}$ is the neighboring state vector of $x_i(t)$, $\Delta P_{d_i}(t) \in R^{k_i}$ is The unpredictable and fluctuating load disturbance is an exogenous disturbance input that is $L_2 \in [0, +\infty)$, and $f_i(x, y) \in R^p$ is a nonlinear function satisfying:

$$f_i^T(x, y) f_i(x, y) \leq \mu x_i^T(t) x_i(t) + \nu y_i^T(t) y_i(t), \quad (4.3)$$

where and are recognised constants, and only one of them may equal zero.. $A_i \in R^{n_i \times n_i}$, $B_i \in R^{n_i \times m_i}$, $C_i \in R^{v_i \times n_i}$, $D_i \in R^{n_i \times l_i}$, $F_i \in R^{n_i \times k_i}$ and $H_i \in R^{n_i \times p_i}$ are known system matrices. $\varpi_i(t)$ Stands for a one-dimensional Brownian motion satisfying and on the probability space (F, P) , where and represent the observed output. It is assumed that the pairs (A_i, B_i) and (A_i, C_i) are respectively observable and controllable, and that the system matrix B_i is of full column rank, i.e. $\text{rank}(B_i) = m_i$. refers to the time-varying system uncertainty, which takes the following form:

$$\tilde{A}_i(t) = J_i G_i(t) M_i \quad (4.4)$$

where $J_i \in R^{n_i \times q_i}$ and $M_i \in R^{r_i \times n_i}$ are constant matrices, and $G_i(t) \in R^{q_i \times r_i}$ is a time-varying matrix satisfying,

$$G_i^T(t) G_i(t) \leq \zeta, \quad (4.5)$$

In which $\zeta = \text{diag}\{\varepsilon_1, \varepsilon_2, \dots, \varepsilon_r\}$ and $\varepsilon_k (k = 1, 2, \dots, r)$ are known constants that means it is a diagonal matrix. Here,

$\tilde{A}_i(t)$ is said to be admissible if equation (4.4) and (4.5) are satisfied simultaneously for all $t \geq 0$. the study model of the i^{th} area of multi-area interconnected power system model with stochastic perturbation as shown in Fig. 4.1.

The integral formula of Itô is used to solve the stochastic differential equation [56].

$$d \Delta f_i(t) = \left[\begin{array}{l} -\frac{1}{T_{P_i}} \Delta f_i(t) + \frac{K_{P_i}}{T_{P_i}} \Delta P_{g_i}(t) - \frac{K_{P_i}}{T_{P_i}} \Delta P_{d_i}(t) + \\ \frac{1}{K_{E_i}} w_i(t) - \frac{K_{P_i}}{2\pi T_{P_i}} \sum_{\substack{j \in N \\ j \neq i}} K_{sij} \{ \Delta \delta_i(t) - \Delta \delta_j(t) \} \end{array} \right] dt + \Theta_{i1}(t) \quad (4.6)$$

$$d \Delta P_{g_i}(t) = \left[-\frac{1}{T_{T_i}} \Delta P_{g_i}(t) + \frac{1}{T_{T_i}} \Delta X_{g_i}(t) \right] dt + \Theta_{i2}(t) \quad (4.7)$$

$$d \Delta X_{g_i}(t) = \left[-\frac{1}{R_i T_{G_i}} \Delta f_i(t) - \frac{1}{T_{G_i}} \Delta X_{g_i}(t) - \frac{1}{T_{G_i}} \Delta E_i(t) + \frac{1}{T_{G_i}} u_i(t) \right] dt + \Theta_{i3}(t) \quad (4.8)$$

$$d \Delta E_i(t) = K_{E_i} \left[K_{B_i} \Delta f_i(t) + \frac{1}{2\pi} \sum_{\substack{j \in N \\ j \neq i}} K_{sij} \{ \Delta \delta_i(t) - \Delta \delta_j(t) \} \right] dt + \Theta_{i4}(t) \quad (4.9)$$

$$d \Delta \delta_i(t) = [2\pi f_i(t)] dt + \Theta_{i5}(t) \quad (4.10)$$

where, $i=1, \dots, N$ is the number of area.

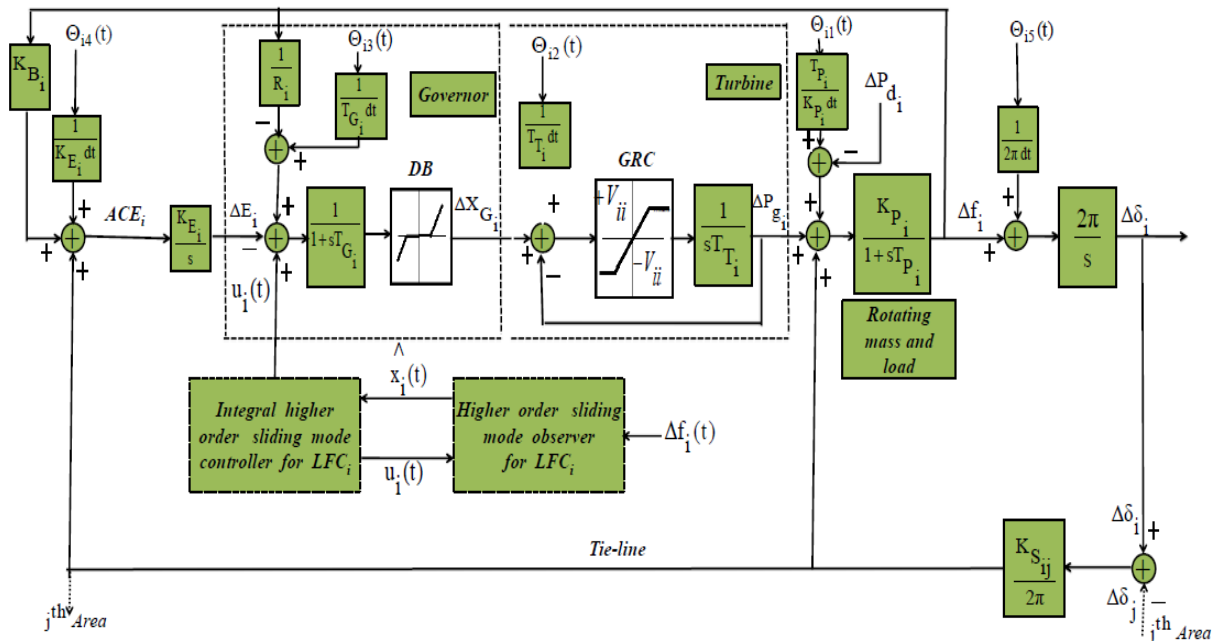


Fig. 4.1 The *i*th area power system's block diagram with stochastic disturbance

$$A_i = \begin{bmatrix} -\frac{1}{T_{P_i}} & \frac{K_{P_i}}{T_{P_i}} & 0 & 0 & -\frac{K_{P_i}}{2\pi T_{P_i}} \sum_{\substack{j \in N \\ j \neq i}} K_{sij} \{\Delta\delta_j(t) - \Delta\delta_i(t)\} \\ 0 & -\frac{1}{T_{T_i}} & \frac{1}{T_{T_i}} & 0 & 0 \\ -\frac{1}{R_i T_{G_i}} & 0 & \frac{1}{T_{G_i}} & -\frac{1}{T_{G_i}} & 0 \\ K_{E_i} K_{B_i} & 0 & 0 & 0 & \frac{K_{E_i}}{2\pi} \sum_{\substack{j \in N \\ j \neq i}} K_{sij} \\ 2\pi & 0 & 0 & 0 & 0 \end{bmatrix}$$

$$B_i = \begin{bmatrix} 0 & 0 & \frac{1}{T_{G_i}} & 0 & 0 \end{bmatrix}^T ; \quad F_i = \begin{bmatrix} -\frac{K_{P_i}}{T_{P_i}} & 0 & 0 & 0 & 0 \end{bmatrix}^T ;$$

$$D_i = \begin{bmatrix} \frac{1}{K_{E_i}} & 0 & 0 & 0 & 0 \end{bmatrix}^T ; \quad H_i = \begin{bmatrix} \frac{1}{K_{E_i}} & 1 & 1 & 1 & 1 \\ 1 & 1 & 1 & 1 & 1 \\ \frac{1}{10 K_{P_i}} & 1 & 1 & 1 & 1 \\ 1 & 1 & 1 & 1 & 1 \\ 1 & 1 & 1 & 1 & 1 \end{bmatrix} ;$$

$$H_i f_i(x(t), y(t)) d\varpi_i(t) = \begin{bmatrix} \Theta_{i1}(t) \\ \Theta_{i2}(t) \\ \Theta_{i3}(t) \\ \Theta_{i4}(t) \\ \Theta_{i5}(t) \end{bmatrix} \quad w_i(t) = 0.01 \sin(t)$$

$$E_{ij} = \begin{bmatrix} 0 & 0 & 0 & 0 & -\frac{K_{P_i}}{2\pi T_{P_i}} K_{sij} \\ 0 & 0 & 0 & 0 & 0 \\ 0 & 0 & 0 & 0 & 0 \\ 0 & 0 & 0 & 0 & -\frac{K_{E_i}}{2\pi} K_{sij} \\ 2\pi & 0 & 0 & 0 & 0 \end{bmatrix}; \quad x_i(t) = \begin{bmatrix} \Delta f_i(t) \\ \Delta P_{g_i}(t) \\ \Delta X_{g_i}(t) \\ \Delta E_i(t) \\ \Delta \delta_i(t) \end{bmatrix};$$

Variables $\Delta f_i(t)$, $\Delta P_{g_i}(t)$, $\Delta X_{g_i}(t)$, $\Delta E_i(t)$, and $\Delta \delta_i(t)$ regarding the alterations in frequency, power output, the location of the governor valve, integral control, and rotor angle deviation, respectively; The time constants for the governor, turbine, and power system are TG, TTi, and TPi, respectively. The power system gain, speed regulation coefficient, integral control gain, and frequency bias factor are KPi, Ri, KEi, and KBi, respectively. The connectivity gain between areas i and j is called KSij. If the exchange power between areas i and j is zero, then KSij=0. The multi-area power system dynamic model with matrices representing parameter uncertainty.

$$dx_i(t) = \begin{bmatrix} \left(A_i + \tilde{A}_i(t) \right) x_i(t) + \left(B_i + \tilde{B}_i(t) \right) u_i(t) + \\ D_i w_i(t) + \sum_{\substack{j \in N \\ j \neq i}} E_{ij} x_j(t) + \left(F_i + \tilde{F}_i(t) \right) \Delta P_{d_i}(t) \end{bmatrix} dt + H_i f_i(x(t), y(t)) d\varpi_i(t) \quad (4.11)$$

where $\tilde{A}_i(t) \in R^{n_i \times n_i}$, $\tilde{B}_i(t) \in R^{n_i \times m_i}$, and $\tilde{F}_i(t) \in R^{n_i \times k_i}$ are uncertainty parameters. For simplification uncertainty is not considered in Brownian white noise and interconnection term E_{ij} .

Let $a_i(t) = \tilde{A}_i(t)x_i(t) + \tilde{B}_i(t)u_i(t) + \left(F_i + \tilde{F}_i(t) \right) \Delta P_{d_i}(t)$ is the aggregated uncertainty, (4.11) becomes as:

$$dx_i(t) = \begin{bmatrix} A_i x_i(t) + B_i u_i(t) + D_i w_i(t) + \\ \sum_{\substack{j \in N \\ j \neq i}} E_{ij} x_j(t) \end{bmatrix} dt + H_i f_i(x(t), y(t)) d\varpi_i(t) + a_i(t) dt \quad (4.12)$$

To guarantee the sliding surface's asymptotic stability, the following presumptions are made; these relate to both the overall system and the proposed controller:

Assumption 1: The pairs (A_i, B_i) and (A_i, C_i) are fully controllable and observable, respectively.

Assumption 2: The matching condition is true given as:

$$a_i(t) = B_i a'_i(t) \quad (4.13)$$

where, $a'_i(t) \in R^{m_i}$.

Assumption 3: The aggregated disturbance $a'_i(t)$ bounded, such that $\|a'_i(t)\| \leq \lambda_i$, where $\| \cdot \|$ is matrix norm and λ_i is known scalar.

Parameters values of three area system model given as [28]:

Table 4.1 System parameter values of three area system model

Area	T_{Pi}	K_{Pi}	T_{Ti}	T_{Gi}	R_i	K_{Ei}	K_{Bi}	K_{Sij}
1	21	125	0.4	0.09	3.2	11	0.45	0.66
2	24	145.32	0.44	0.0785	2.7	8	0.38	0.67
3	21	151	0.35	0.07	2.6	7.5	0.4	0.56

2.1. Design of observer based sliding mode controller

Without the stochastic disturbance $d\varpi(t)$, A system's state will eventually return to its initial state asymptotically. Disturbances cause the states of a system to wander erratically, but still remain confined by a region that is close to their origin. Using the information, we have about the disturbance; we aim to design a sliding surface that will lessen its impact on the disturbance $d\varpi(t)$. For the sake of simplicity, we assume the following and consider the disturbance to be a stochastic process.

Assumption 1: The disturbance is bounded, i.e. $\sup_{0 \leq t \leq \infty} |d\varpi(t)| \leq \varphi$, Where φ , is a positive real number and $\varphi \neq 0$.

Assumption 2: $d\varpi(t)$ is a stationary, distribution of $\{d\varpi(t_1 + t), d\varpi(t_2 + t), \dots, d\varpi(t_n + t)\}$ is independent on time t .

Assumption 3: $t_n \neq t_{n+1} \Rightarrow d\varpi(t_n)$ and $d\varpi(t_{n+1})$ both are independent.

2.2. higher order sliding mode observer design

In the process of establishing control laws terms have the advantage of avoiding conventional low pass filters. They also have the disadvantage of making the output dependent on the integrator output. The system will be adversely affected if noise levels are reduced. In [58] and [59], Theorem 8 proved that the observation error can be reduced to zero in a finite amount of time. By performing a coordinate transformation on the system, it is possible to represent the observer as a matrix;

$$\dot{\hat{x}}_i = A_i \hat{x}_i(t) + B_i u_i(t) + z_i(t) \quad (4.14)$$

where $z_i(t)$ is the correction term [58].

$$\begin{aligned} \dot{\hat{x}}_1(t) &= \zeta_1 \\ \zeta_1 &= \hat{x}_2(t) + \bar{g}_1(x_1, u) - \lambda_1 \Gamma^{n+1} |\hat{x}_1(t) - x_1(t)|^{\frac{n}{n+1}} \operatorname{sgn}(\hat{x}_1(t) - x_1(t)) \\ \dot{\hat{x}}_2(t) &= \zeta_2 \\ \zeta_2 &= \hat{x}_3(t) + \bar{g}_2(x_1, \hat{x}_2, u) - \lambda_2 \Gamma^n |\hat{x}_2(t) - \zeta_1|^{\frac{n-1}{n}} \operatorname{sgn}(\hat{x}_2(t) - \zeta_1) \\ \dot{\hat{x}}_n(t) &= \zeta_n \\ \zeta_n &= \bar{f}_n(\hat{x}) + g_n(x, \hat{x}, u) - \lambda_n \Gamma^2 |\hat{x}_n(t) - \zeta_{n-1}|^{\frac{1}{2}} \operatorname{sgn}(\hat{x}_n(t) - \zeta_{n-1}) \quad (4.15) \end{aligned}$$

An additional source that can be used for the development of a higher order sliding mode observer is [58]. An asymptotic estimate of the states can be made by a higher order sliding mode observer. $\hat{x}_i(t)$ in the system and satisfies the following condition as:

$$\lim_{t \rightarrow \infty} \left\| \hat{x}_i(t) - x_i(t) \right\| = 0 \quad (4.16)$$

$$\left(\int_a^b x^T(t) dt \right) P \left(\int_a^b x(t) dt \right) \leq (b-a) \int_a^b x^T(t) P x(t) dt \quad (4.17)$$

2.3. Design of sliding surface and formulation of control law

This paragraph discussed how an integrated sliding surface might be used for an unexpected power system. Control techniques such as sliding mode control, often referred to as SMC, have been proven to be reliable and effective for managing unpredictable nonlinear systems [60–64]. A discontinuous system control is used by SMC in order to move the system state trajectory to a predetermined sliding surface. On these surfaces, the system possesses the desirable characteristics of stability, the capacity to reject shocks, and the ability to track. The sliding surface is one of the relatively independent components of the classic SMC design, and it also has an equivalent control scheme for the intended performance and a controller law to drive the system trajectory to the surface and maintain forward motion on the sliding surface.

$$s_i(t) = G_i \hat{x}_i(t) - \int_0^t G_i \left[(A_i - B_i K_i) - B_i L_i C_i \right] \hat{x}_i(\tau) d\tau \quad (4.18)$$

where $G_i \in R^{m_i \times n_i}$ and $K_i \in R^{m_i \times n_i}$ are known constant matrices. $L_i \in R^{m_i \times v_i}$ a well-known gain. The pole placement technique is used to construct the matrix controller gain so that the matrix's Eigen values are negative. The matrix is chosen in a such that. Because the solution, which can be determined from [65], is likewise a semi-martingale, it can be seen that the sliding surface is a semi-martingale. The sliding surface function meets the following condition as the dynamic trajectory approaches the sliding mode condition, which is as follows: $s_i(t) = 0$ And $\dot{s}_i(t) = 0$

Taking one times derivative of equation (4.14) and two times derivative of equation (4.18) we get,

$$\ddot{\hat{x}}_i(t) = A_i \dot{\hat{x}}_i(t) + B_i \dot{u}_i(t) + \dot{z}_i(t) \quad (4.19)$$

where $\dot{z}_i(t)$ is the correction term of higher order sliding mode observer [58].

$$\ddot{s}_i(t) = G_i \ddot{\hat{x}}_i(t) - G_i \left[(A_i - B_i K_i) \dot{\hat{x}}_i(t) - B_i L_i C_i \dot{\hat{x}}_i(t) \right] \quad (4.20)$$

Substitute the value of equation (4.19) in equation (4.20),

$$\ddot{s}_i(t) = G_i \left(A_i \dot{\hat{x}}_i(t) + B_i \dot{u}_i(t) + \dot{z}_i(t) \right) - G_i \begin{bmatrix} (A_i - B_i K_i) \dot{\hat{x}}_i(t) - \\ B_i L_i C_i \dot{\hat{x}}_i(t) \end{bmatrix} \quad (4.21)$$

New sliding surface is offered for second order integral sliding mode control as,

$$s_{new}(t) = \dot{s}_{old}(t) + \Psi s_{old}(t) \quad (4.22)$$

where, it is considered that

$$s_{iold}(t) = s_i(t) = G_i \hat{x}_i(t) - \int_0^t G_i [(A_i - B_i K_i) \hat{x}_i(\tau) - B_i L_i C_i \hat{x}_i(\tau)] d\tau$$

On differentiating equation (4.19) we get,

$$\dot{s}_{inew}(t) = \dot{s}_{iold}(t) \dot{s}_{iold}(t) + \Psi s_{iold}(t) \quad (4.23)$$

Now, substitute the value of equation (4.19) in equation (4.21),

$$\dot{s}_{inew}(t) = G_i \left(A_i \dot{\hat{x}}_i(t) + B_i \dot{u}_i(t) + \dot{z}_i(t) \right) - G_i \begin{bmatrix} (A_i - B_i K_i) \dot{\hat{x}}_i(t) - \\ B_i L_i C_i \dot{\hat{x}}_i(t) \end{bmatrix} + \Psi s_{iold}(t) \quad (4.24)$$

By the constant rate reaching law of sliding mode controller $\dot{s}_{inew}(t)$ is replaced by $\dot{s}_{inew}(t) = -\beta \operatorname{sgn}(s_{inew})$ in above equation. Based on observer after solving we get the following equivalent control law for stochastic system;

$$u_i(t) = - \left\{ \begin{array}{l} K_i \dot{\hat{x}}_i(t) + L_i C_i \dot{\hat{x}}_i(t) + B_i^{-1} \dot{z}_i(t) + \\ B_i^{-1} G_i^{-1} \Psi s_{iold}(t) + B_i^{-1} G_i^{-1} \beta \operatorname{sgn} \left(s_{iold}(t) + \Psi s_{iold}(t) \right) \end{array} \right\} \quad (4.25)$$

and are well-known non-negative real valued scalars.

Thus, by substituting to obtain the sliding mode dynamics (4.25) into (4.14);

$$\dot{\hat{x}}_i(t) = (A_i - B_i K_i) \hat{x}_i(t) - B_i L_i C_i \hat{x}_i(t) - G_i^{-1} \Psi s_{iold}(t) - \int G_i^{-1} \beta \operatorname{sgn} \left(s_{iold}(t) + \Psi s_{iold}(t) \right) dt \quad (4.26)$$

The sliding motion given in (4.26) is analyzed for its robustness and stochastic stability in the following subsection, and some adequate conditions are derived using the linear matrix inequality approach. Since the dynamics of the observer state are related to the dynamics of the sliding motion (4.21), the stability of the total system, which includes the states and, is being studied rather than the stability of the observer (4.15) alone. In (4.27), an examination of the total closed-loop system that was produced is offered.

3. Stability analysis of overall closed-loop system

The stability study of the entire closed-loop system is covered in this section. The following augmented system can be formulated from (4.1) and (4.15) as follows:

$$dA_i(t) = \left[\begin{array}{l} (A_i + A_{d_i})A_i(t) + B_i e_i(t) + \\ D_i w_i(t) + \sum_{\substack{j \in N \\ j \neq i}} E_{ij} A_j(t) + a_i(t) \end{array} \right] dt + H_i f_i(x(t), y(t)) d\varpi_i(t) \quad (4.27)$$

were,

$$A_i = \begin{bmatrix} A_i & 0_{n_i \times n_i} \\ 0_{n_i \times n_i} & A_i - B_i K_i \end{bmatrix}, \quad A_{d_i} = \begin{bmatrix} -B_i L_i C_i & 0_{n_i \times n_i} \\ 0_{n_i \times n_i} & -B_i L_i C_i \end{bmatrix},$$

$$B_i = \begin{bmatrix} -z_i & 0_{n_i \times n_i} \\ 0_{n_i \times 1} & 0_{n_i \times n_i} \end{bmatrix}, \quad D_i = \begin{bmatrix} D_i \\ 0_{n_i \times l_i} \end{bmatrix}, \quad E_{ij} = \begin{bmatrix} E_{ij} & 0_{n_i \times n_i} \\ 0_{n_i \times n_i} & 0_{n_i \times n_i} \end{bmatrix},$$

$$e_i(t) = \begin{bmatrix} 1 \\ 0_{n_i \times n_i} \end{bmatrix}, \quad a_i(t) = \begin{bmatrix} a_i(t) \\ 0_{n_i \times 1} \end{bmatrix}, \quad A_i(t) = \begin{bmatrix} [x_i(t) - \hat{x}_i(t)]^T & \hat{x}_i(t)^T \end{bmatrix},$$

$$H_i = \begin{bmatrix} H \\ 0_{n_i \times p_i} \end{bmatrix},$$

The criterion of robust stochastic stability is given in Theorem 1 [56].

Theorem 4.1 For given scalars $\mu \geq 0$, $\nu \geq 0$, $\rho \geq 0$, and $\delta \geq 0$, pre-defined matrices $L_i \in R^{m_i \times v_i}$ and $K_i \in R^{m_i \times n_i}$ in (4.18), under higher order sliding mode control (4.25) is robust stochastically stable with H_∞ performance level γ if there exists a scalar $\beta > 0$, positive definite matrices $\Omega_1 \in R^{\nu \times \nu}$, $\Omega_2 \in R^{n \times n}$, $Q_x \in R^{n \times n}$, $R_x \in R^{n \times n}$, Matrices $S_{yz} \in R^{2n \times 2n}$, $S_{y5} \in R^{(v+n) \times 2n}$ and $S_{y6} \in R^{l \times 2n}$ ($x = 1, 2, \dots, 6$ and $y, z = 1, 2, \dots, 4$) such that

$$\Xi < 0, \quad (4.28)$$

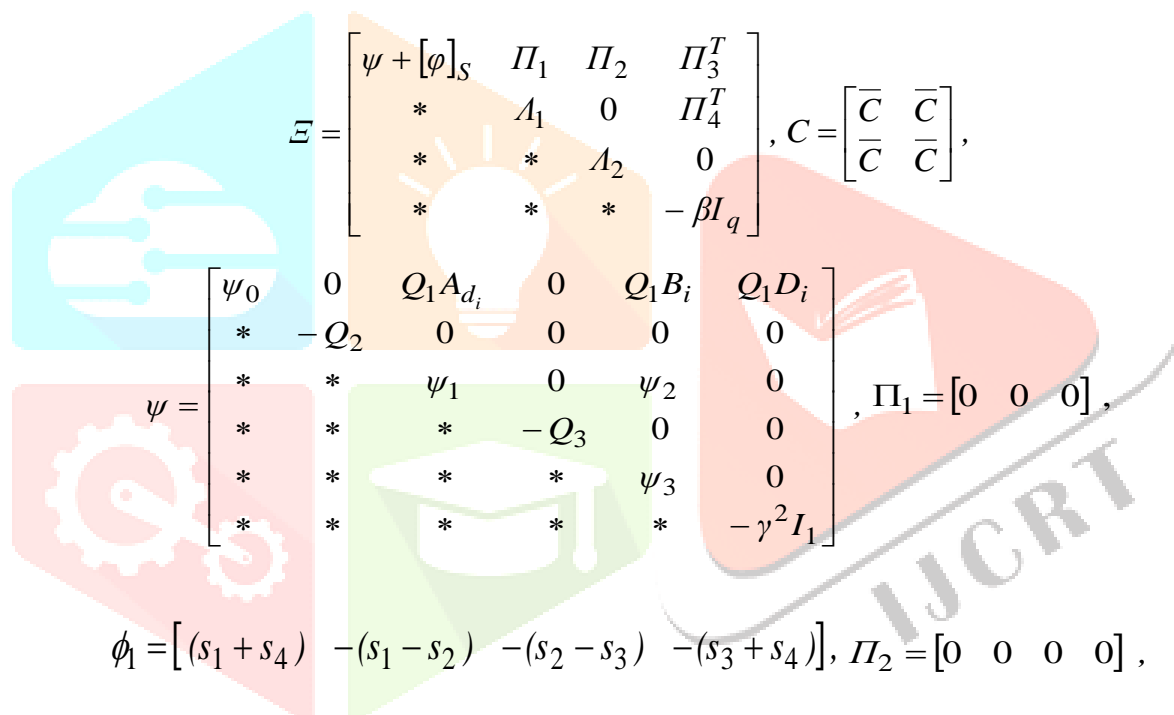
$$H_i^T Q_1 H_i - \rho I \leq 0, \quad (4.29)$$

were,

$$\bar{C} = \mu \rho I_n + (v v + 1) C_i^T C_i,$$

$$\psi_0 = [Q_1 A_i]_S + Q_2 + Q_3 + C_i + \beta M_i^T \Lambda M_i,$$

$$\Phi = [\Phi_1 \quad 0_{(v+n) \times (v+n)} \quad 0_{l \times l}],$$



$$\Xi = \begin{bmatrix} \psi + [\varphi]_S & \Pi_1 & \Pi_2 & \Pi_3^T \\ * & A_1 & 0 & \Pi_4^T \\ * & * & A_2 & 0 \\ * & * & * & -\beta I_q \end{bmatrix}, \quad C = \begin{bmatrix} \bar{C} & \bar{C} \\ \bar{C} & \bar{C} \end{bmatrix},$$

$$\psi = \begin{bmatrix} \psi_0 & 0 & Q_1 A_{d_i} & 0 & Q_1 B_i & Q_1 D_i \\ * & -Q_2 & 0 & 0 & 0 & 0 \\ * & * & \psi_1 & 0 & \psi_2 & 0 \\ * & * & * & -Q_3 & 0 & 0 \\ * & * & * & * & \psi_3 & 0 \\ * & * & * & * & * & -\gamma^2 I_1 \end{bmatrix}, \quad \Pi_1 = [0 \quad 0 \quad 0],$$

$$\phi_1 = [(s_1 + s_4) \quad -(s_1 - s_2) \quad -(s_2 - s_3) \quad -(s_3 + s_4)], \quad \Pi_2 = [0 \quad 0 \quad 0 \quad 0],$$

$$\Pi_3 = [J_i^T Q_1 \quad 0 \quad 0 \quad 0 \quad 0 \quad 0], \quad \Pi_4 = [0 \quad 0 \quad 0], \quad Q_x = \text{diag}\{Q_x, R_x\}$$

$$A_1 = \text{diag}\{-Q_4, -Q_5, -Q_6\}, \quad A_2 = \text{diag}\{-Q_4, -Q_5, -Q_5, -Q_6\},$$

$$\psi_1 = \delta [C_i \quad C_i]^T \Omega_1 [C_i \quad C_i] + \delta [0_{n \times n} \quad I_n]^T \Omega_2 [0_{n \times n} \quad I_n],$$

$$\psi_2 = \delta [C_i \quad C_i]^T \Omega_1 [I_v \quad 0_{v \times n}] + \delta [0_{n \times n} \quad I_n]^T \Omega_2 [0_{n \times v} \quad I_n],$$

$$\psi_3 = \delta [I_v \quad 0_{v \times n}]^T \Omega_1 [I_v \quad 0_{v \times n}] + \delta [0_{n \times v} \quad I_n]^T \Omega_2 [0_{n \times v} \quad I_n] - [I_v \quad 0_{v \times n}]^T \Omega_1 [I_v \quad 0_{v \times n}] - [0_{n \times v} \quad I_n]^T \Omega_2 [0_{n \times v} \quad I_n] \quad (4.30)$$

Proof. The Lyapunov functional candidate is selected as [35]:

$$V_1(t) = \sum_{x=1}^6 V_{1x}(t), \quad (4.31)$$

$$\text{With } V_{11}(t) = A_i^T(t)Q_1A_i(t), \quad V_{12}(t) = \int A_i^T(s)Q_2A_i(s)ds,$$

$$V_{13}(t) = \int A_i^T(s)Q_3A_i(s)ds, \quad V_{14}(t) = \iint \theta_i^T(s)Q_4\theta_i(s)dsdv,$$

$$V_{15}(t) = \iint \theta_i^T(s)Q_5\theta_i(s)dsdv, \quad V_{16}(t) = \iint \theta_i^T(s)Q_6\theta_i(s)dsdv,$$

$$\text{where } \theta_i(t) = (A_i + A_{d_i})A_i(t) + B_i e_i(t) + D_i w_i(t) + \sum_{\substack{j \in N \\ j \neq i}} E_{ij} A_j(t) + a_i(t),$$

$$\text{With } \theta_i(t) \in R^{2n},$$

Using stochastic differential equations' operational characteristics in [56].

$$E\{LV_{11}(t)\} = E\left\{2A_i^T(t)Q_1\theta_i(t) + f_i^T(t)H_iQ_1H_i f_i(t)\right\},$$

$$E\{LV_{12}(t)\} = E\left\{A_i^T(t)Q_2A_i(t) - A_i^T(t)Q_2A_i(t)\right\} = E\{0\},$$

$$E\{LV_{13}(t)\} = E\left\{A_i^T(t)Q_3A_i(t) - A_i^T(t)Q_3A_i(t)\right\} = E\{0\},$$

$$E\{LV_{14}(t)\} = E\left\{0 - \int \theta_i^T(s)Q_4\theta_i(s)ds\right\},$$

$$E\{LV_{15}(t)\} = E\left\{0 - \int \theta_i^T(s)Q_5\theta_i(s)ds\right\},$$

$$E\{LV_{16}(t)\} = E\left\{0 - \int \theta_i^T(s)Q_6\theta_i(s)ds\right\},$$

Introduce the following slack matrices for $x = 1, 2, 3, 4$

$$S_i = \begin{bmatrix} S_{i1}^T & S_{i2}^T & S_{i3}^T & S_{i4}^T & S_{i5}^T & S_{i6}^T \end{bmatrix}^T.$$

Recalling $E\{d\varpi_i(t)\} = 0$ and using the Leibnitz-Newton formula [65], we get,

$$0 = E\left\{2\xi_i^T(t)S_1(0 - \int \theta_i(s)ds)\right\},$$

$$0 = E \left\{ 2 \xi_i^T(t) S_2 (0 - \int \theta_i(s) ds) \right\},$$

$$0 = E \left\{ 2 \xi_i^T(t) S_3 (0 - \int \theta_i(s) ds) \right\},$$

$$0 = E \left\{ 2 \xi_i^T(t) S_4 (0 - \int \theta_i(s) ds) \right\}, \quad (4.32)$$

where,

$$\xi_i(t) = \begin{bmatrix} \xi_1^T(t) & A_i^T(t) & e_i^T(t) & w_i^T(t) \end{bmatrix}^T,$$

$$\xi_1(t) = \begin{bmatrix} A_i^T(t) & A_i^T(t) & A_i^T(t) \end{bmatrix}^T,$$

In addition, by assuming that; according to Lemma 5,

$$\xi_i^T(t) S_1 \int \theta_i(s) ds = \int \xi_i^T(t) S_1 \theta_i(s) ds,$$

We have,

$$-2 \xi_i^T(t) S_1 \int \theta_i(s) ds \leq \int \theta_i^T(s) Q_4 \theta_i(s) ds \quad (4.33)$$

$$-2 \xi_i^T(t) S_2 \int \theta_i(s) ds \leq \int \theta_i^T(s) Q_5 \theta_i(s) ds \quad (4.34)$$

$$-2 \xi_i^T(t) S_3 \int \theta_i(s) ds \leq \int \theta_i^T(s) Q_5 \theta_i(s) ds \quad (4.35)$$

$$-2 \xi_i^T(t) S_4 \int \theta_i(s) ds \leq \int \theta_i^T(s) Q_6 \theta_i(s) ds \quad (4.36)$$

From (4.29) and (4.3), we obtained,

$$f_i^T(x(t), y(t)) H_i^T Q_1 H_i f_i(x(t), y(t)) \leq \rho \left(\mu x_i^T(t) x_i(t) + \nu y_i^T(t) y_i(t) \right), \quad (4.37)$$

First, we take performance into account and create the following index, which is,

$$T < E \left\{ \xi_i^T(t) (\bar{\Psi} + [\Phi]_S) \xi_i(t) \right\}, \quad (4.38)$$

where

$$\bar{\Psi} = \begin{bmatrix} \bar{\psi}_0 & 0 & Q_1 A_{d_i} & 0 & Q_1 B_i & Q_1 D_i \\ * & -Q_2 & 0 & 0 & 0 & 0 \\ * & * & \psi_1 & 0 & \psi_2 & 0 \\ * & * & * & -Q_3 & 0 & 0 \\ * & * & * & * & \psi_3 & 0 \\ * & * & * & * & * & -\gamma^2 I \end{bmatrix},$$

$$\bar{\psi}_0 = \left[Q_1 \left(A_i + \tilde{A}_i(t) \right) \right]_S + Q_2 + Q_3 + C_i, \quad (4.39)$$

And Ψ_1, Ψ_2, Ψ_3 and Φ are defined in (4.30).

Apply Schur complement in (4.28), we have $\tilde{\Xi} + \beta M_i^T \zeta M_i + \zeta^{-1} \Pi_5^T \Pi_5 < 0$ where

$$\tilde{\psi} = \begin{bmatrix} \tilde{\psi}_0 & 0 & Q_1 A_{d_i} & 0 & Q_1 B_i \\ * & -Q_2 & 0 & 0 & 0 \\ * & * & \psi_1 & 0 & \psi_2 \\ * & * & * & -Q_3 & 0 \\ * & * & * & * & \psi_3 \end{bmatrix},$$

$$\bar{M}_i = [M_i \ 0 \ 0 \ 0 \ 0 \ 0 \ 0 \ 0 \ 0],$$

$$\tilde{\Xi} = \begin{bmatrix} \tilde{\psi} + [\Phi]_S & \Pi_1 & \Pi_2 \\ * & \zeta_1 & 0 \\ * & * & \zeta_2 \end{bmatrix}, \quad \tilde{\psi}_0 = [Q_1 A_i]_S + Q_2 + Q_3,$$

$$\Pi_5 = [\Pi_{51} \ 0 \ 0 \ 0], \quad \Pi_{51} = [J_i^T Q_1 \ 0 \ 0 \ 0 \ 0 \ 0],$$

Now, according to Proposition 2.1 in [56], it follows $\Xi < 0$ from

$$\tilde{\Xi} + \beta M_i^T \zeta M_i + \zeta^{-1} \Pi_5^T \Pi_5 < 0, \quad \text{where } \bar{\Xi} = \begin{bmatrix} \bar{\psi} + [\Phi]_S & \bar{\Pi}_1 & \Pi_2 \\ * & \zeta_1 & 0 \\ * & * & \zeta_2 \end{bmatrix}, \quad \bar{\Pi}_1 = [0 \ 0 \ 0], \quad \text{and } \bar{\psi} \text{ are defined}$$

in (4.39). By using Schur complement, we have,

$$\bar{\psi} + [\Phi]_S < 0,$$

This implies that,

$$E\{LV_i(t) + y^T(t)y(t) - \gamma^2 w_i^T(t)w_i(t)\} < 0.$$

The result of integrating the previous inequality from 0 to $+\infty$ is

$$E\left\{ \int_0^{+\infty} y^T(t)y(t)dt - \int_0^{+\infty} \gamma^2 w_i^T(t)w_i(t)dt \right\} < E\{V_1(0) - \ell\} \leq 0,$$

where $V_1(0) = 0$ and $V_1(+\infty) \geq 0$. In other condition under disturbance free case, $E\{LV_i(t)\} < 0$ from (4.28)-(4.29) by setting $w_i(t) = 0$ for system (4.27). Overall, the robust stochastic stability in sense may be assured with proposed controller (4.25), in accordance with definition 1 for all allowable uncertainties of the system.

4. Simulation and Results

Using a composite higher order observer-based second order sliding mode controller and a standard SMC in the face of exogenous, unpredictable load variation and stochastic perturbation, a time-domain MATLAB simulation of the LFC design for multi area power system is described in this study. The frequency variation in real life may be 1% Hz. To determine the viability of the suggested control strategy, a three-area linked power system [28] is examined. The characteristics that make a person in authority The system's mathematical model is displayed in Table I. This model has some flaws when compared to the actual plant. It is caused by mathematical approximation, unmodeled dynamics, and disregarding the impact of various forms of certain and uncertain disruptions. As the operational circumstances of the power system change, parameter uncertainty may result. Following system parameter changes are conducted to show the suggested controller's robustness:

$$\begin{aligned}
T_{T1} &\in [0.24, 0.36], & T_{G1} &\in [0.064, 0.096], \\
R_1 T_{G1} &\in [0.1229, 0.2765], & T_{T2} &\in [0.264, 0.3960], \\
T_{G2} &\in [0.0576, 0.0864], & R_2 T_{G2} &\in [0.112, 0.252], \\
T_{T3} &\in [0.28, 0.42], & T_{G3} &\in [0.056, 0.084], \\
R_3 T_{G3} &\in [0.112, 0.252].
\end{aligned}$$

The parameters' average values are chosen in. The following are the nominal system models for the three areas:

Area 1:

$$A_1 = \begin{bmatrix} -0.05 & 6 & 0 & 0 & -0.955 \\ 0 & -3.472 & 3.472 & 0 & 0 \\ -5.878 & 0 & -13.021 & -13.021 & 0 \\ 4 & 0 & 0 & 0 & 1.592 \\ 6.283 & 0 & 0 & 0 & 0 \end{bmatrix} \quad F_1 = \begin{bmatrix} -6 \\ 0 \\ 0 \\ 0 \\ 0 \end{bmatrix}$$

$$f_1(x(t), y(t)) = [\sin 0.4x_1(t) \cdot \sin x(t) \quad 0 \quad 0 \quad 0 \quad 0]^T$$

$$E_{13} = \begin{bmatrix} 0 & 0 & 0 & 0 & 0.478 \\ 0 & 0 & 0 & 0 & 0 \\ 0 & 0 & 0 & 0 & 0 \\ 0 & 0 & 0 & 0 & -0.796 \\ 0 & 0 & 0 & 0 & 0 \end{bmatrix} \quad E_{12} = \begin{bmatrix} 0 & 0 & 0 & 0 & 0.478 \\ 0 & 0 & 0 & 0 & 0 \\ 0 & 0 & 0 & 0 & 0 \\ 0 & 0 & 0 & 0 & -0.796 \\ 0 & 0 & 0 & 0 & 0 \end{bmatrix} \quad B_1 = \begin{bmatrix} 0 \\ 0 \\ 13.021 \\ 0 \\ 0 \end{bmatrix}$$

Area 2:

$$A_2 = \begin{bmatrix} -0.04 & 4.5 & 0 & 0 & -0.716 \\ 0 & -3.157 & 3.157 & 0 & 0 \\ -5.805 & 0 & -14.468 & -14.468 & 0 \\ 4 & 0 & 0 & 0 & 1.592 \\ 6.283 & 0 & 0 & 0 & 0 \end{bmatrix} \quad F_2 = \begin{bmatrix} -4.5 \\ 0 \\ 0 \\ 0 \\ 0 \end{bmatrix}$$

$$f_2(x(t), y(t)) = [\sin 0.3x_1(t) \cdot \sin x(t) \quad 0 \quad 0 \quad 0 \quad 0]^T$$

$$E_{21} = \begin{bmatrix} 0 & 0 & 0 & 0 & 0.358 \\ 0 & 0 & 0 & 0 & 0 \\ 0 & 0 & 0 & 0 & 0 \\ 0 & 0 & 0 & 0 & -0.796 \\ 0 & 0 & 0 & 0 & 0 \end{bmatrix} \quad E_{23} = \begin{bmatrix} 0 & 0 & 0 & 0 & 0.358 \\ 0 & 0 & 0 & 0 & 0 \\ 0 & 0 & 0 & 0 & 0 \\ 0 & 0 & 0 & 0 & -0.796 \\ 0 & 0 & 0 & 0 & 0 \end{bmatrix} \quad B_2 = \begin{bmatrix} 0 \\ 0 \\ 14.468 \\ 0 \\ 0 \end{bmatrix}$$

Area 3:

$$A_3 = \begin{bmatrix} -0.05 & 5.75 & 0 & 0 & -0.915 \\ 0 & -2.976 & 2.976 & 0 & 0 \\ -6.448 & 0 & -14.881 & -14.881 & 0 \\ 4 & 0 & 0 & 0 & 1.592 \\ 6.283 & 0 & 0 & 0 & 0 \end{bmatrix} \quad F_3 = \begin{bmatrix} -5.75 \\ 0 \\ 0 \\ 0 \\ 0 \end{bmatrix}$$

$$f_3(x(t),y(t)) = [\sin 0.2x_1(t) \cdot \sin x(t) \quad 0 \quad 0 \quad 0 \quad 0]^T$$

$$E_{31} = \begin{bmatrix} 0 & 0 & 0 & 0 & 0.358 \\ 0 & 0 & 0 & 0 & 0 \\ 0 & 0 & 0 & 0 & 0 \\ 0 & 0 & 0 & 0 & -0.796 \\ 0 & 0 & 0 & 0 & 0 \end{bmatrix} \quad E_{32} = \begin{bmatrix} 0 & 0 & 0 & 0 & 0.458 \\ 0 & 0 & 0 & 0 & 0 \\ 0 & 0 & 0 & 0 & 0 \\ 0 & 0 & 0 & 0 & -0.796 \\ 0 & 0 & 0 & 0 & 0 \end{bmatrix} \quad B_3 = \begin{bmatrix} 0 \\ 0 \\ 14.881 \\ 0 \\ 0 \end{bmatrix}$$

The three-scenario based on uncertain load disturbances, exogenous, stochastic perturbation, systems non-linearity and validation of observer have been investigated while utilising the suggested controller as:

Study 1: In this scenario, the frequency deviation and control signal with step load disturbances with, $\Delta P_{d1} = -0.12$, $\Delta P_{d2} = -0.07$ and $\Delta P_{d3} = -0.05$ is demonstrated with traditional SMC. It has been noted that each area's frequency variation is accompanied by considerable overshoot and settling down the system till 6 second. The high frequency switching control (chattering) causes the mechanical stress in practical implementation which is reduced with the proposed controller and also deviation in frequency settles down till 0.2 second. It also provides minimum undershoot and overshoot as compared to traditional SMC. Further tie-line power deviation and robustness property of controller is validated under step load disturbance with stochastic perturbation. All results for study 1 as shown in Fig. 4.2.

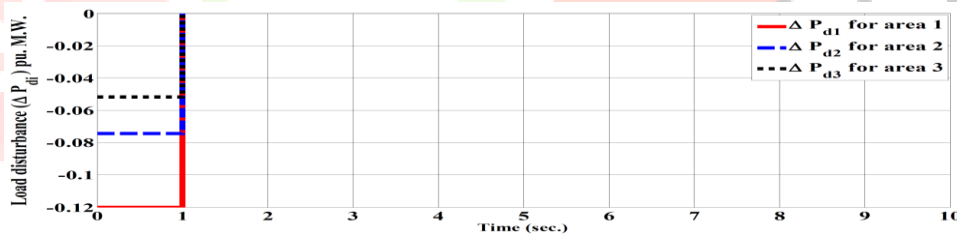


Fig. 4.2 Step load disturbance

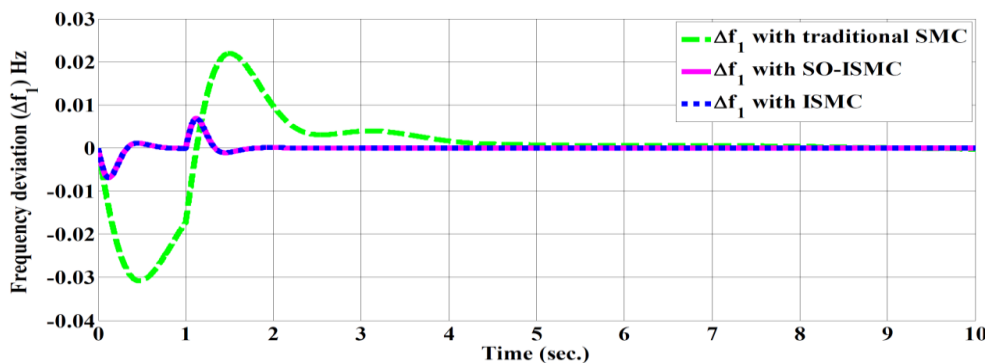


Fig. 4.3 Area 1 of frequency deviation for traditional SMC, SO-ISMC and ISMC

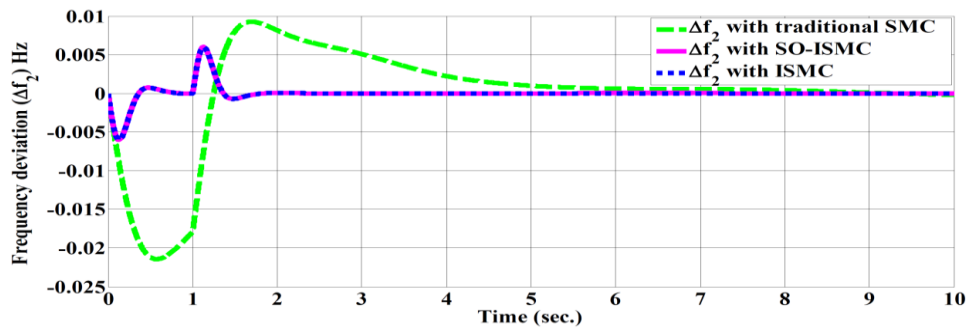


Fig. 4.4 Area 2 of frequency deviation for traditional SMC, SO-ISM and ISMC

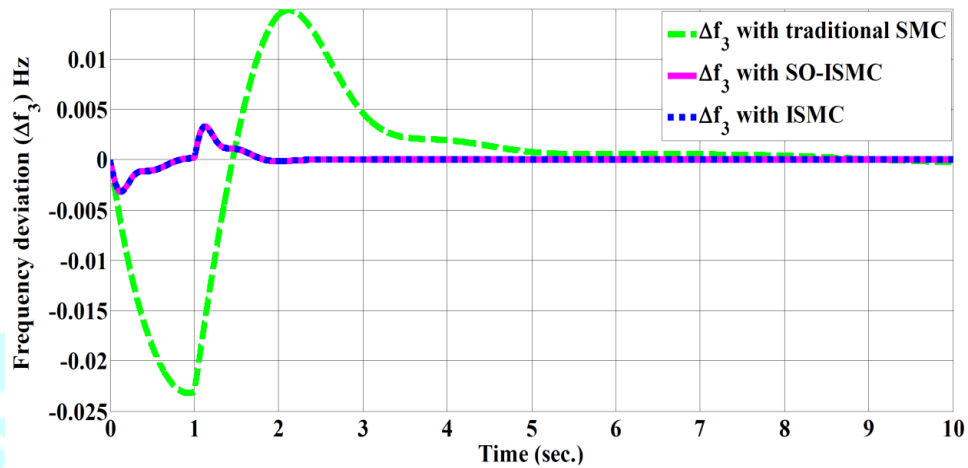


Fig. 4.5 region 3 of the frequency deviation for traditional SMC, SO-ISM and ISMC

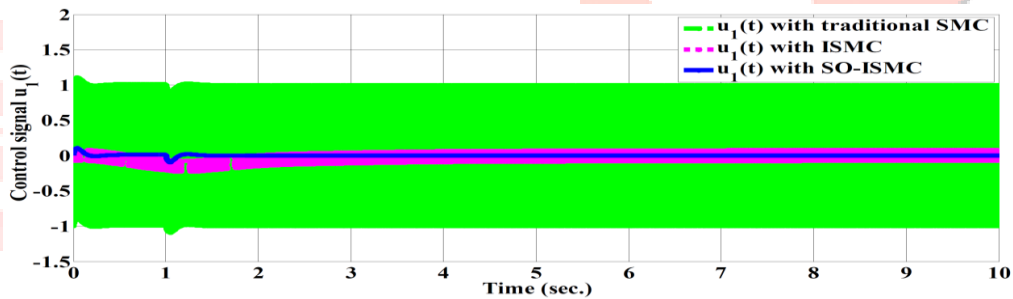


Fig. 4.6 Control signal area 1 for traditional SMC, SO-ISM and ISMC

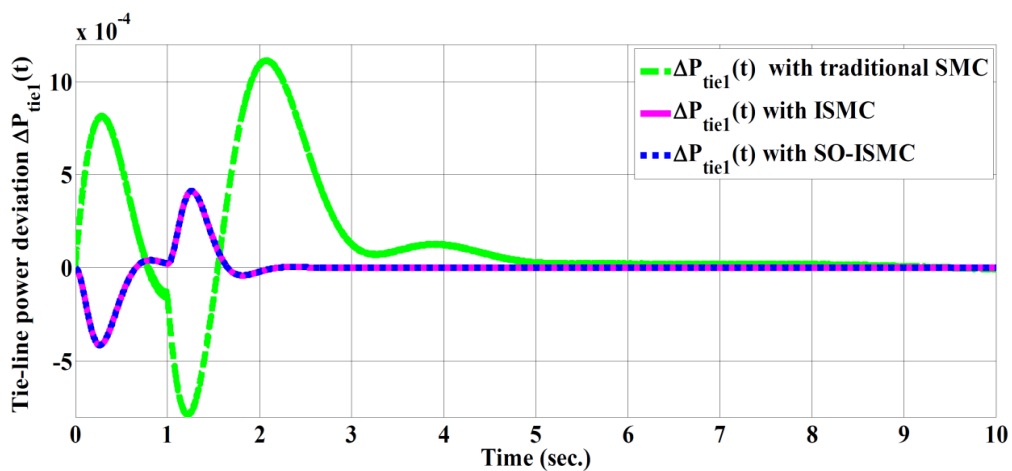


Fig. 4.7 Area 1 of the tie-line power deviation for traditional SMC, SO-ISM and ISMC

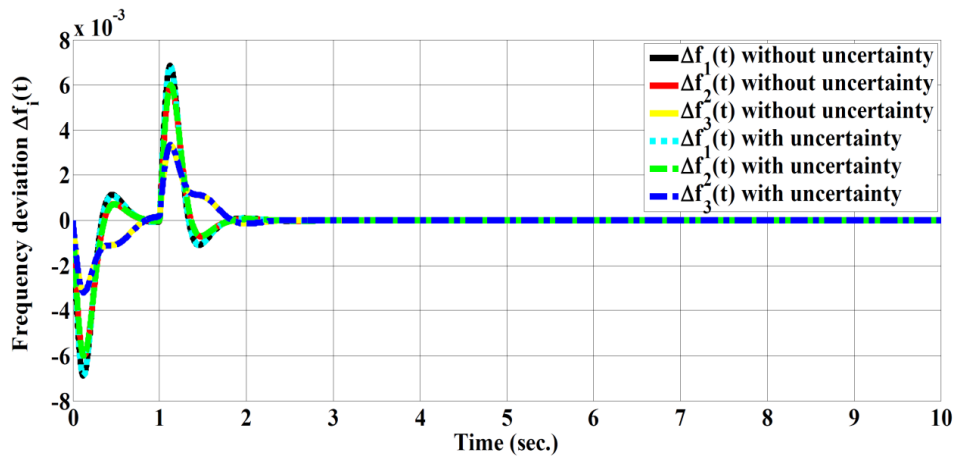


Fig. 4.8 Response for robustness of SO-ISMIC under step load

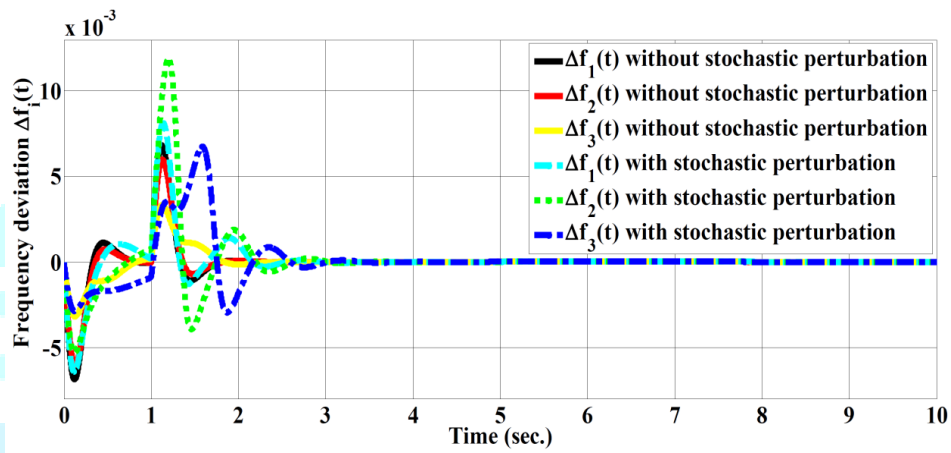


Fig. 4.9 Frequency deviation under step load with stochastic perturbation

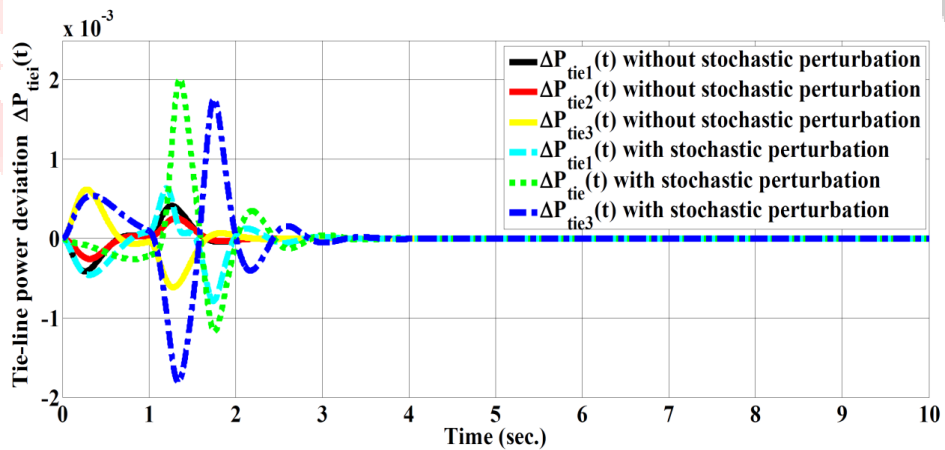


Fig. 4.10 Tie-line power deviation Using step load and stochastic perturbation

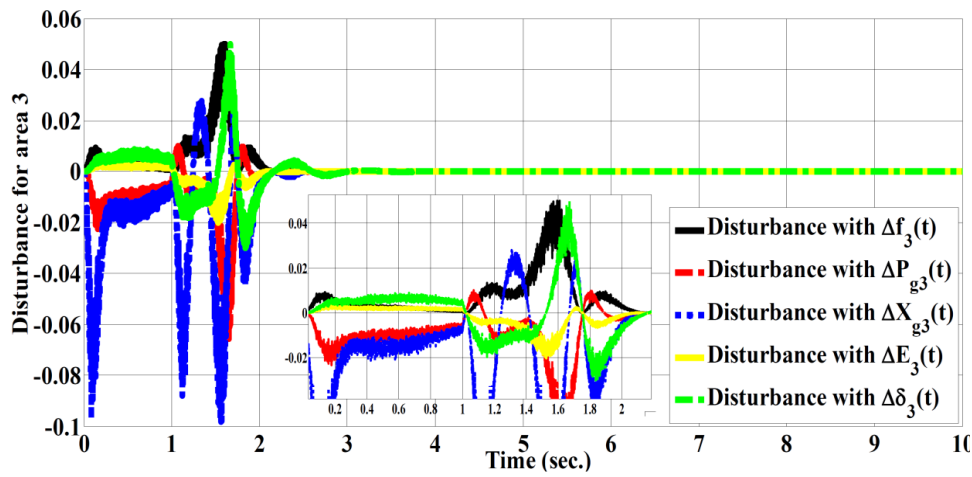


Fig. 4.11 Disturbance for area 3 under step load

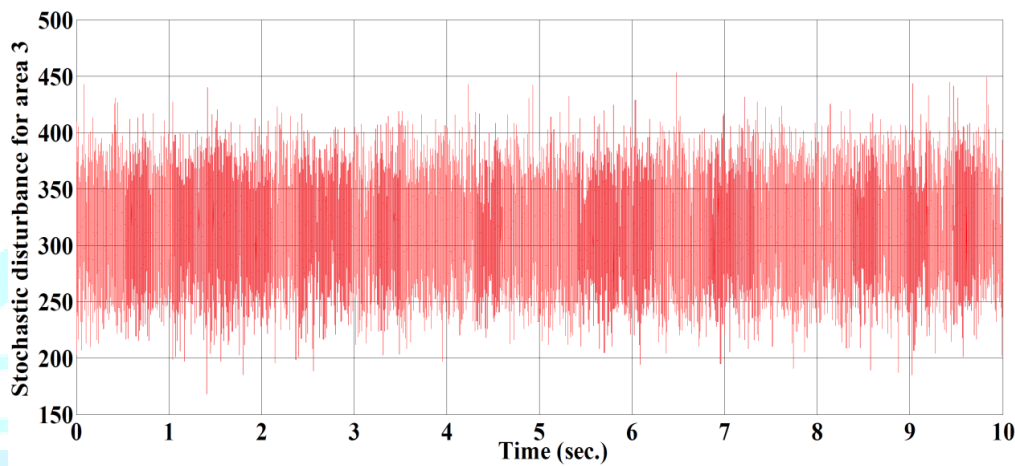


Fig. 4.12 Stochastic disturbance for area 3 under step load

A composite SMC with the following form is tested for robustness using nominal parameters with an uncertain load disturbance and the same time-varying matched parameter uncertainty [56]. Thus, robustness can be assessed.

$$\tilde{A}(t) = JG(t)M$$

$$J = [0 \ 0 \ 0 \ 5 \ 1]^T, M = [0 \ 0 \ 0 \ 1 \ 5], G(t) = 0.1 \sin(t)$$

The $\Delta f_i(t)$ without and with the parameter uncertainty and uncertain varying load disturbance where the suggested controller compensates for the matching uncertainty, validating its robustness and causing it to stabilise fast. The proposed controller considerably reduces the frequency deviation. In light of this, the suggested controller achieves strong performance against uncertainties. With the suggested controller, the tie-line power variations are also reduced under a variety of disturbances and stabilise for up to 2 seconds.

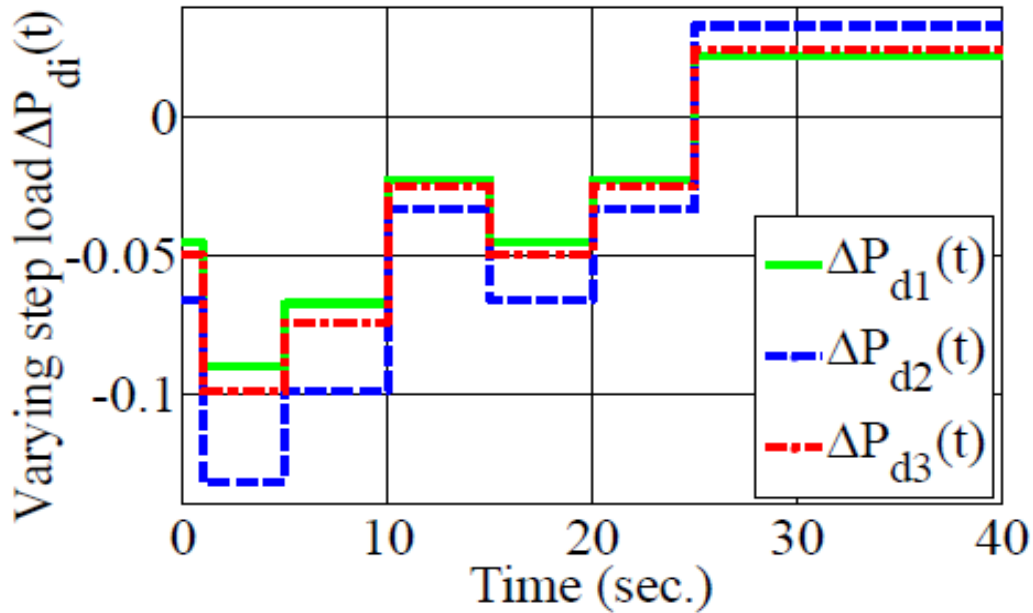


Fig. 4.13 Varying step load disturbance

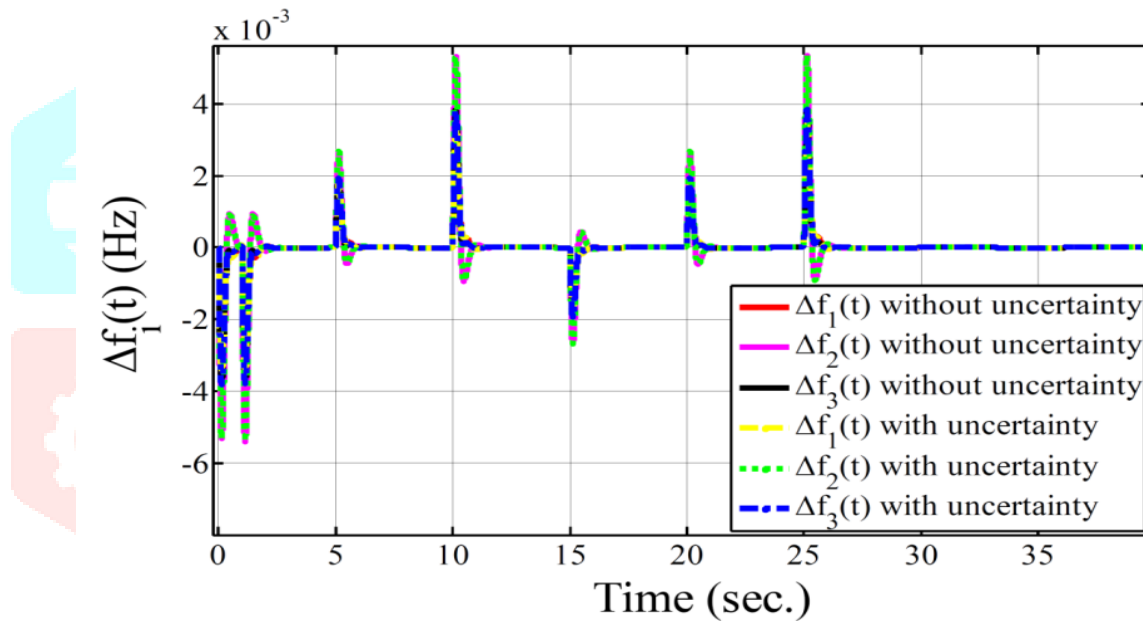


Fig. 4.14 Response for robustness of controller under varying step disturbance

Study 2: This subsection is discussed with inclusion of systems nonlinearities a generation rate limitation (GRC), for instance. having its limits [28]. Another non-linearity dead

The governor operation introduces a band with a 0.06pu limit [54]. Below is a depiction of the frequency deviation achieved using the suggested control approach with dead band and GRC. This one shows how the proposed controller performs satisfactorily, leading the frequency deviation profile to be established quickly.

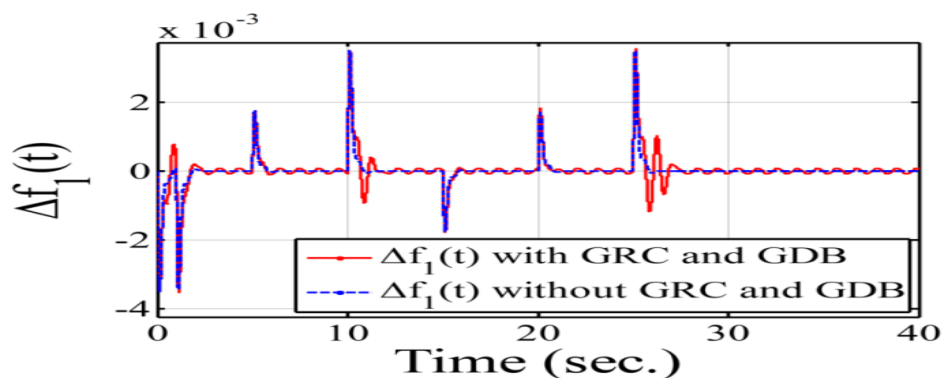


Fig. 4.15 Area 1 of frequency variation using GRC and GDB

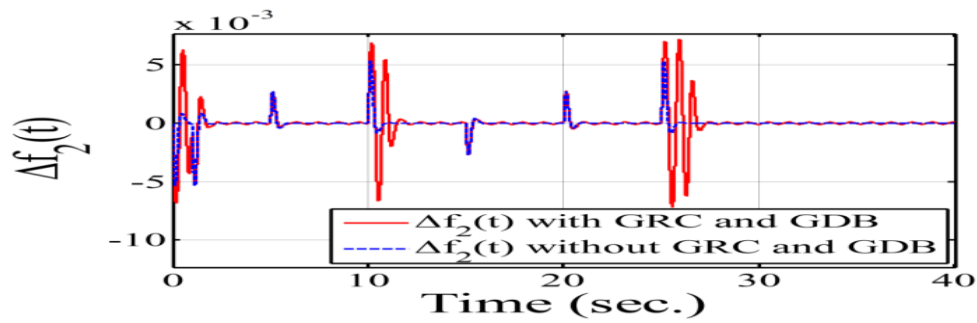


Fig. 4.16 Area 2 of the frequency variation with GRC and GDB

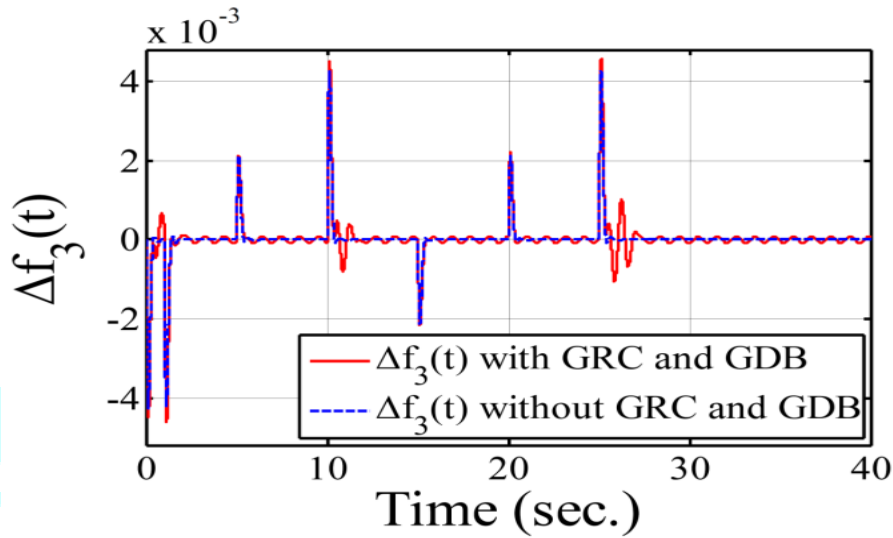


Fig. 4.17 Area of frequency deviation 3 with GRC and GDB

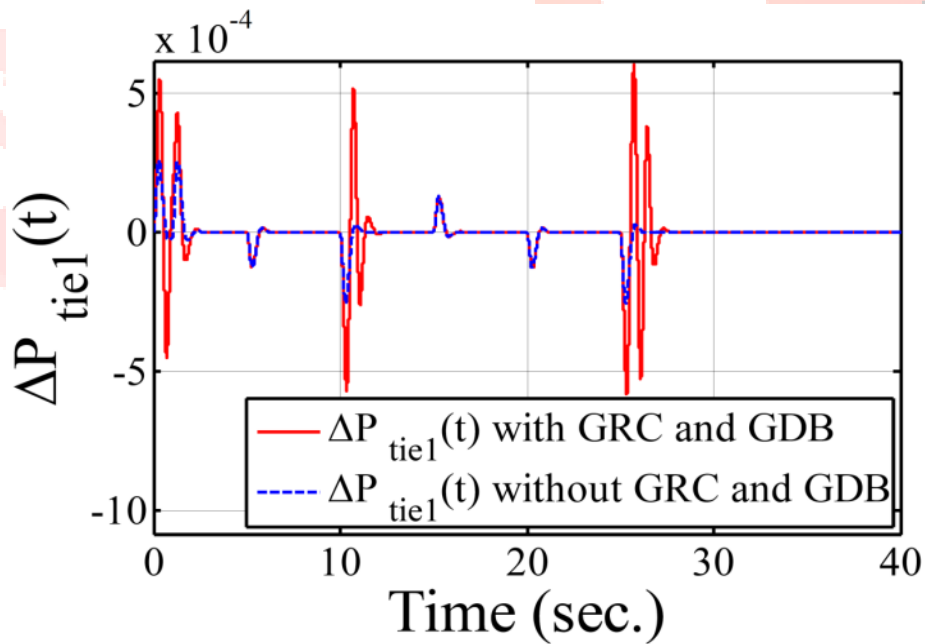


Fig. 4.18 region 1 of the tie-line power deviation GRC and GDB

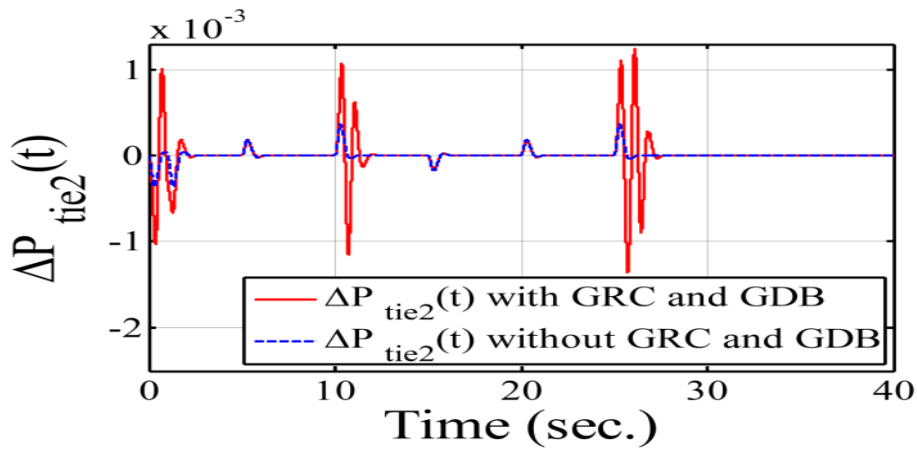


Fig. 4.19 Area 2 of the tie-line power deviation GRC and GDB

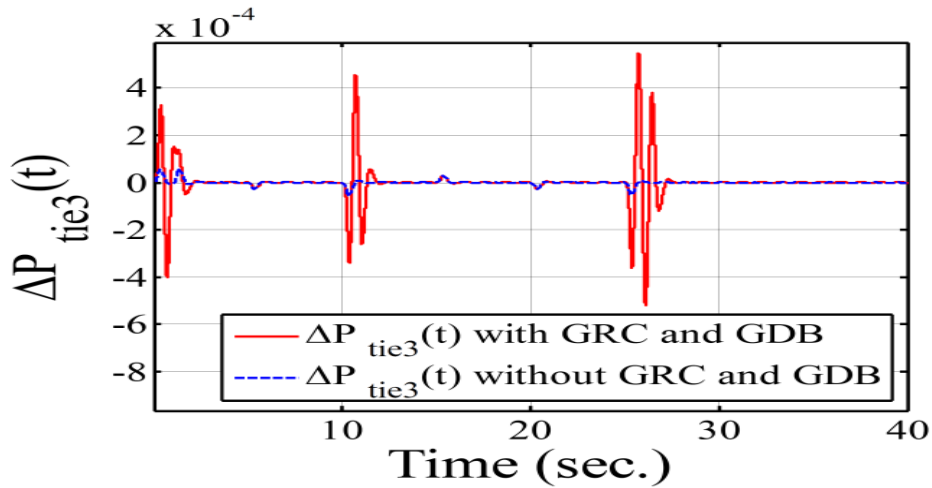


Fig. 4.20 Area 3 of the tie-line power deviation with GRC and GDB

Study 3: The deterministic dynamic network model combined with the stochastic load fluctuation model is considered to reduce the discrepancy between actual plant and its approximated mathematical model. The proposed controller provides the improved performance for this practical plant.

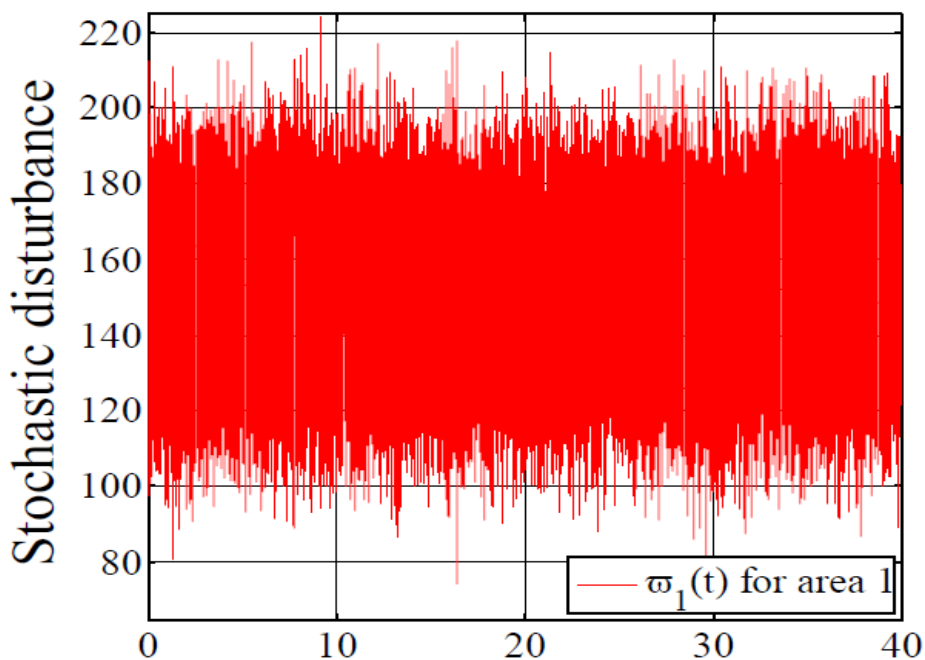


Fig. 4.21 Stochastic disturbance for area 1

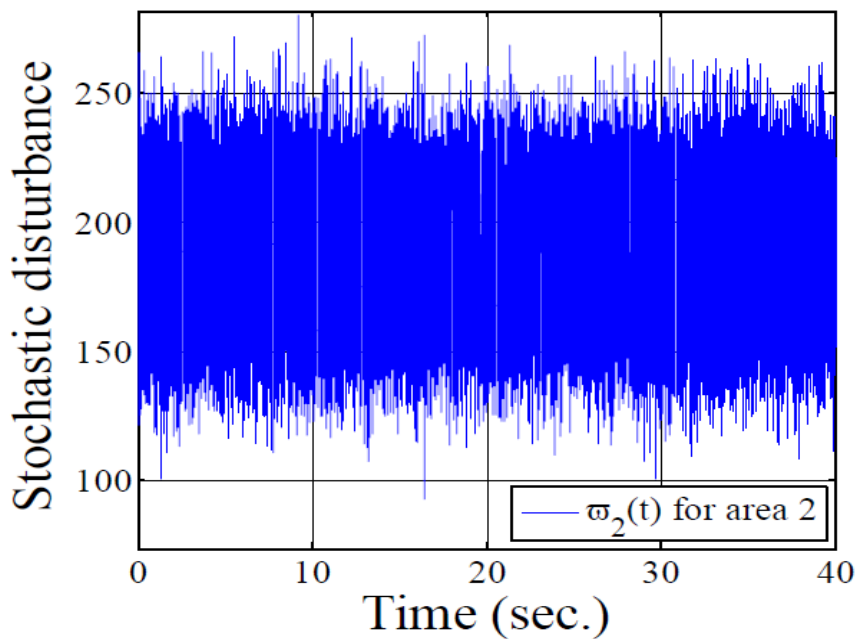


Fig. 4.22 Stochastic disturbance for area 2

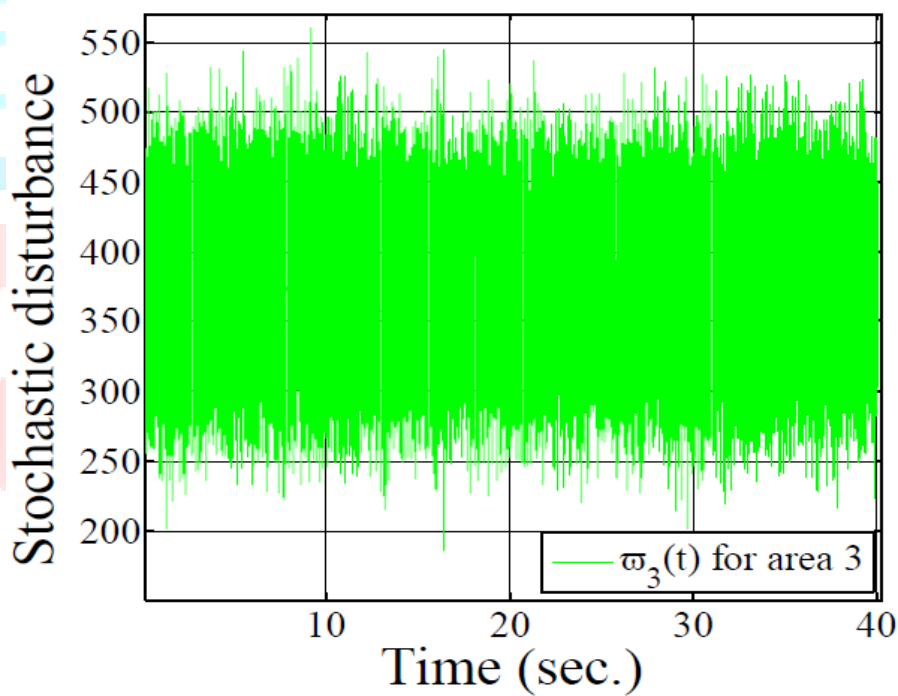


Fig. 4.23 Stochastic disturbance for area 3

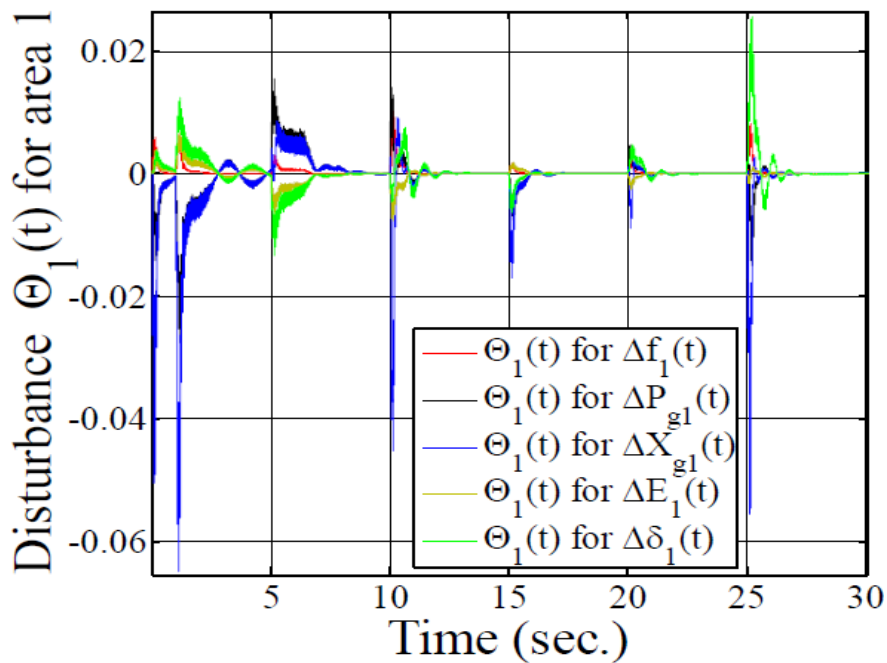


Fig. 4.24 Disturbance for area 1

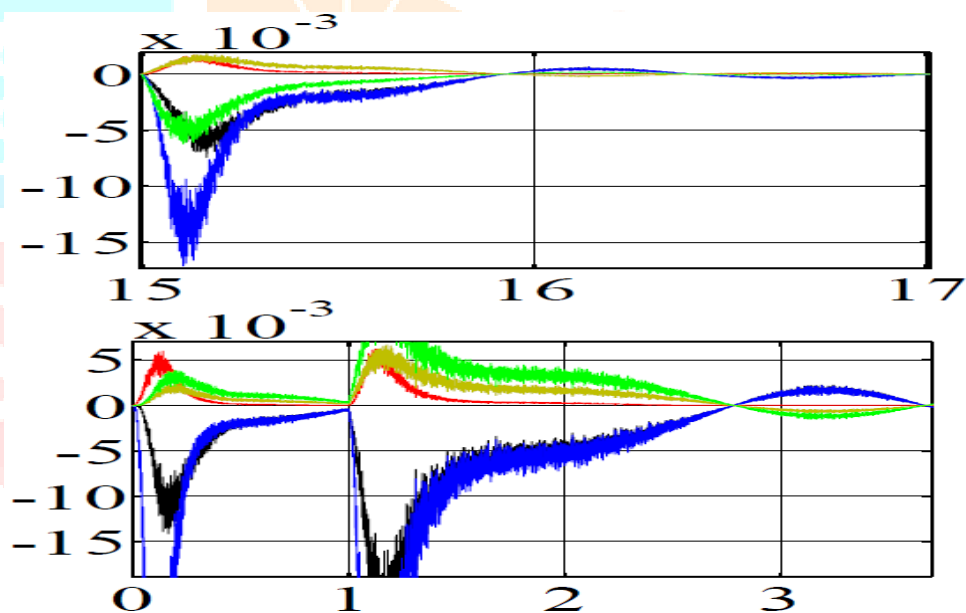


Fig. 4.25 Zoom plot of Fig. 4.24

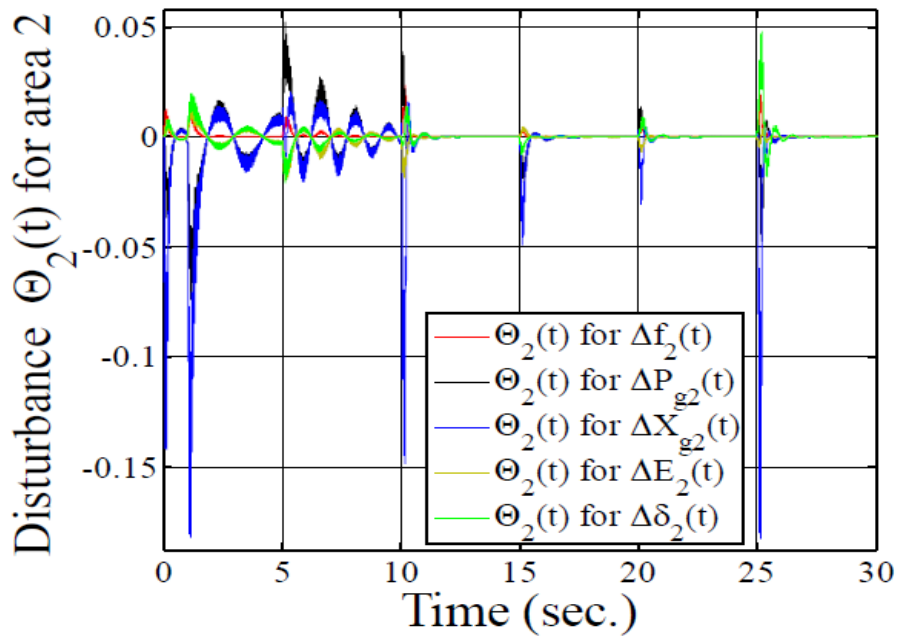


Fig. 4.26 Disturbance for area 2

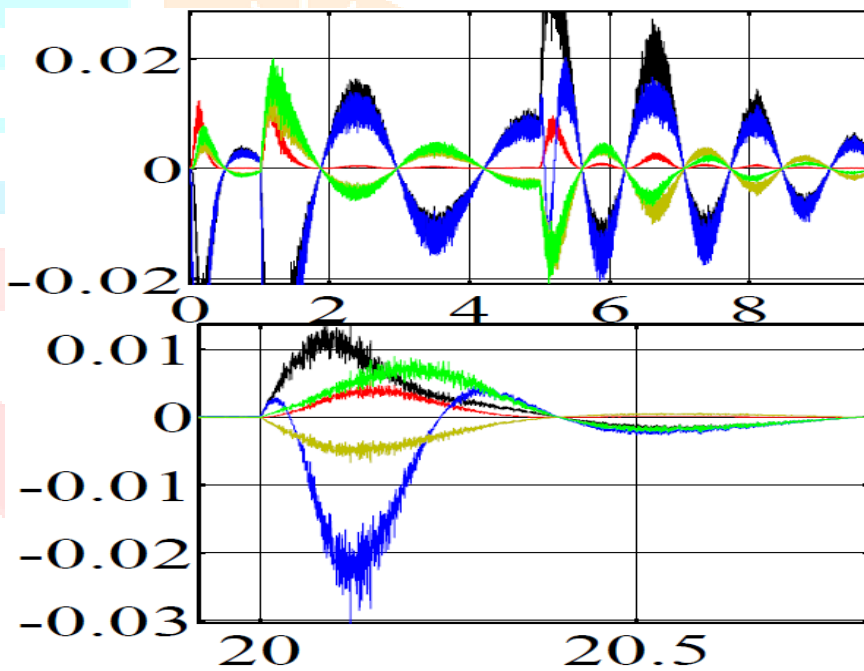


Fig. 4.27 Zoom plot of Fig. 4.26

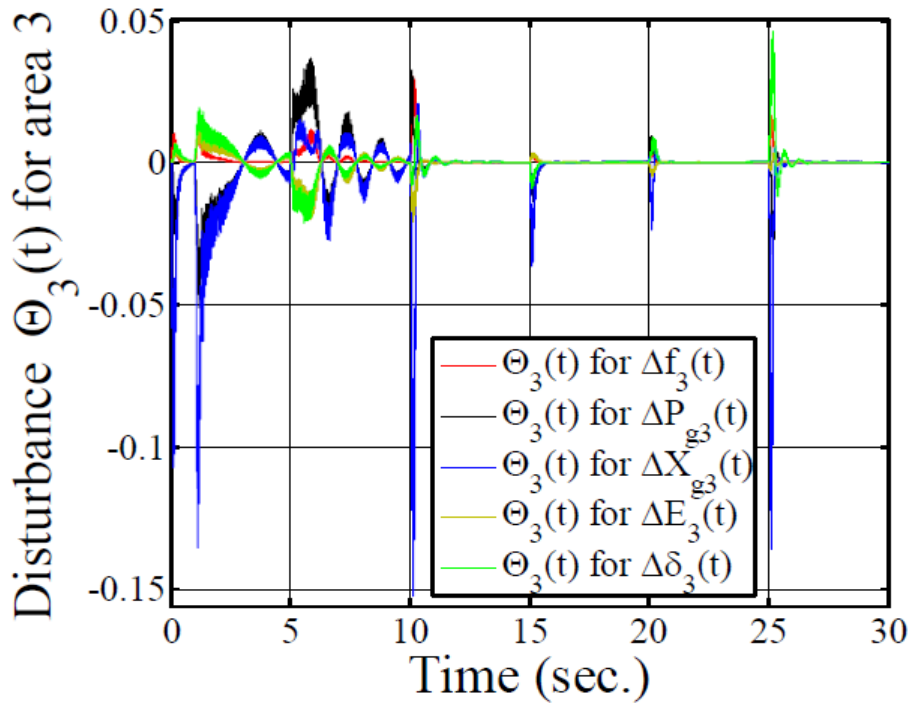


Fig. 4.28 Disturbance for area 3

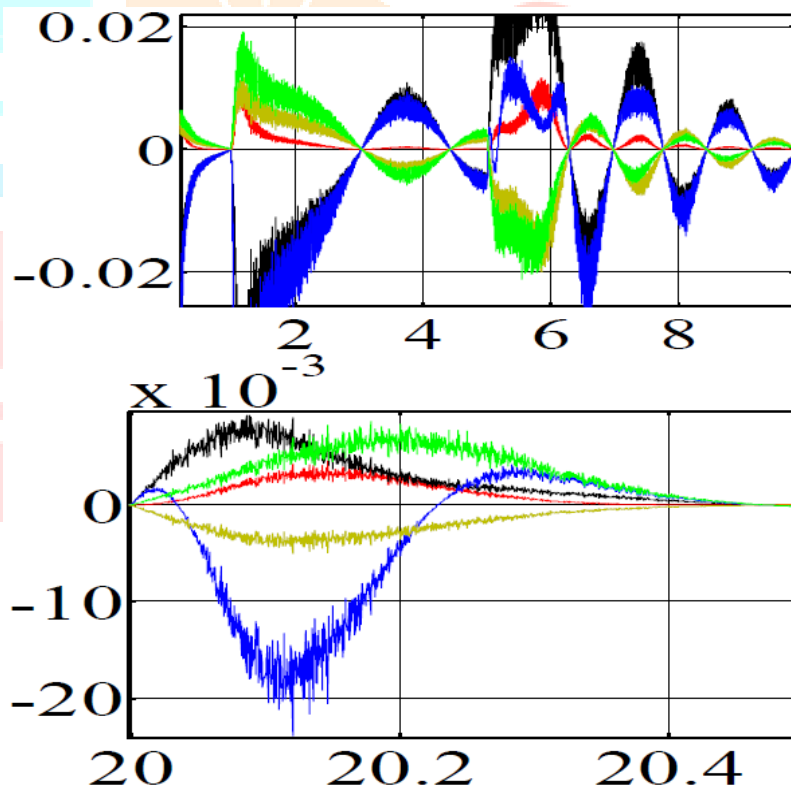


Fig. 4.29 Zoom plot of Fig. 4.28

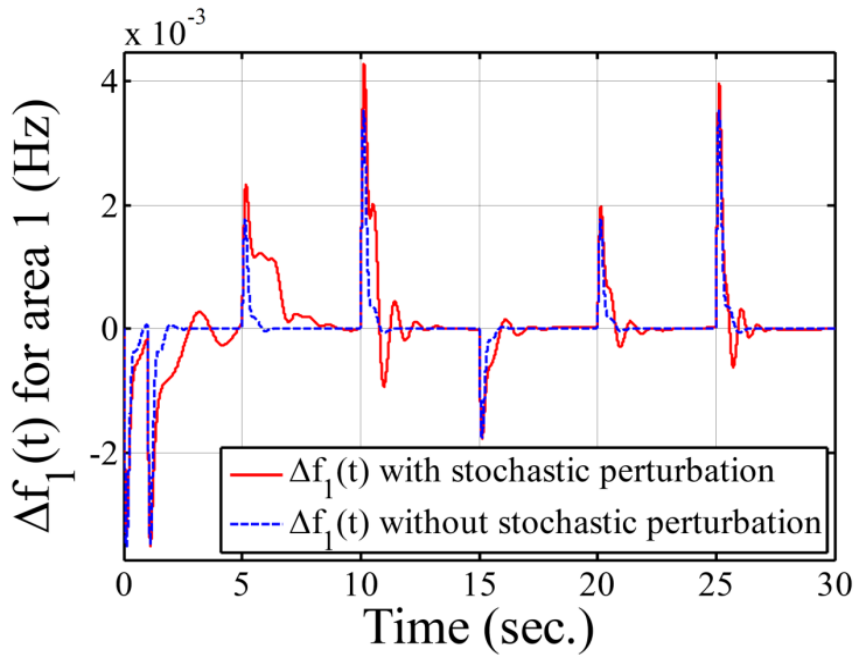


Fig. 4.30 Frequency deviation area 1 with stochastic perturbation

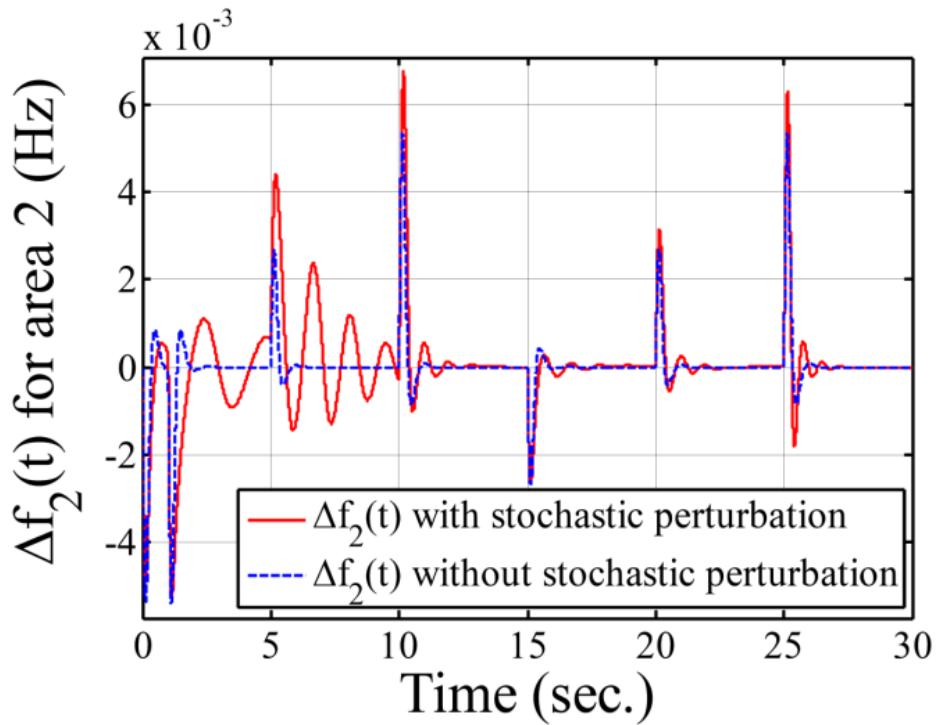


Fig. 4.31 Frequency deviation area 2 with stochastic perturbation

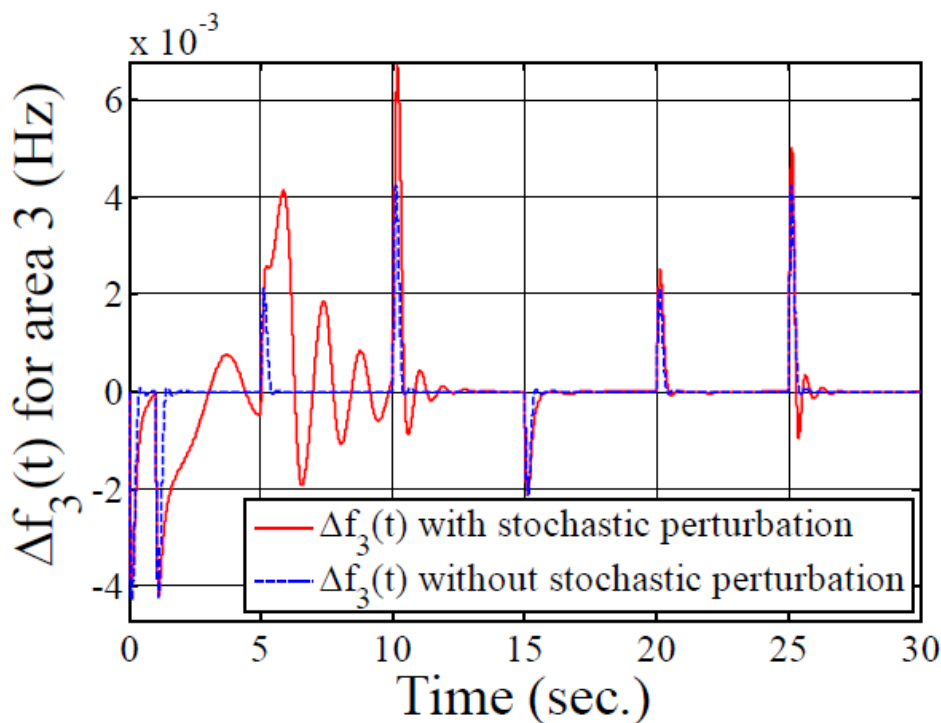


Fig. 4.32 Frequency deviation area 3 with stochastic perturbation

5. Conclusion

In this conclusion we develop higher order sliding mode controls for uncertain systems that are susceptible to external disturbances, stochastic perturbations, load disturbances, and parameter uncertainties. The aforementioned factors can make it difficult to control these types of systems. The research begins with an introduction to variable structure control, specifically sliding mode control. It is a nonlinear control approach with a high degree of dependability. Traditionally, sliding mode control is hampered by unwanted chattering in the control signal, which limits its applicability to real-world applications and affects its efficiency. Almost always, chattering in the control signal results in poor control accuracy, increased wear and tear on moving mechanical components, and increased heat accumulation in power circuits. There are several functions that can be used to approximate a discontinuous control signal's signum function, including saturation, sigmoid, tanh, etc. We discuss some preliminary concepts and ideas that inspired us to create sliding mode control in this paper. We compare the resilience of a linear approximation sliding mode controller with that of a sigmoid approximation sliding mode controller. Here, a higher order sliding mode controller is used to eliminate the chattering present in the control signal. As a result, the controller's robustness property is maintained. We develop a higher order sliding mode observer in this article using sensors to estimate the highly unpredictable states of the system. Unlike sliding mode observers, higher order sliding mode observers do not require filters. Using a higher order sliding mode controller, a chatter-free control signal is provided in this research. Using the controller, the case study deals with load frequency difficulties for multiple region power systems. In this study we evaluate the proposed controller's ability to withstand disturbances of various kinds, such as load disturbances, external disturbances, unclear parameter values, stochastic Brownian noise, etc. Observer-based higher order sliding mode control for load frequency difficulties is tested using generation rate constant (GRC) and governor dead band system nonlinearities as test subjects.

5.1. Scope for Future Work

- ❖ Design of observer based integral higher order sliding mode control with input saturation nonlinearity to trace the nonlinear control signal.
- ❖ in future work will address nonlinear signal tracing and actuator saturation flight control
- ❖ The proposed method would be applied for multi-input and multi-output system with input saturation nonlinearity.

REFERENCES

1. I. Ibraheem, P. Kumar and D. P. Kothari, "Recent philosophies of automatic generation control strategies in power systems", IEEE Transition Power System, vol. 20, no. 1, pp. 346–357, 2005.
2. C. Gardiner, "Handbook of stochastic methods", Springer Berlin, 1985.
3. M. Majid, H. A. Rahman and O. Jais, "Study of fuzzy logic power system stabilizer", 2002.
4. M. L. Kothari, K. Bhattacharya and J. Nanda, "Adaptive power system stabilizer based on pole shifting technique", IEEE proceedings, vol. 143, pp. 96-98, 1993.
5. F. Rashidi, M. Rashidi and H. Amiri, "An adaptive fuzzy sliding mode control for power system stabilizer", Industrial Electronics Society, IECON'03. The 29th Annual Conference of the IEEE, pp. 625-630, Nov. 2003.
6. G. P. Chen and O. P. Malik, "Optimization technique for the design of a linear optimal power system stabilizer", IEEE Trans. on Energy Conversion, vol. 7, no. 3, Sept. 1992.
7. Z. M. A. Hamouz and Y. L. AbdeI-Magid, "Variable structure load frequency controllers for multi area power systems", Elect. Power Energy Syst., vol. 15, no. 5, pp. 293–300, Feb. 1993.
8. M. Zribi, M. A. Rashed and M. Alrifai, "Adaptive decentralized load frequency control of multi-area power systems", Elect. Power Energy Syst., vol. 27, no. 8, pp. 575–583, Oct. 2005.
9. K. Y. Lim, Y. Wang and R. Zhou, "Robust decentralised load-frequency control of multi-area power systems", Proc. Inst. Elect. Eng., Gener., Transm., Distrib., vol. 143, no. 5, pp. 377–386, Sept. 1996.
10. M. A. Rifai and M. Zribi, "A robust decentralized controller for power system load frequency control", in Proc. Universities Power Engineering Conf., vol. 3, pp. 794–799, Sept. 2004.
11. P. Kundur, "Power System Stability and Control", New York, NY, USA: McGraw-Hill, 1994.
12. R. Goshaidas, D. Sitansu and T. K. Bhattacharyyam, "Multi-area load frequency control of power systems: A decentralized variable structure approach", Elect. Power Compon. Syst., vol. 33, no. 3, pp. 315–331, Oct. 2004.
13. H. Bevrani and T. Hiyama, "Robust decentralized PI based LFC design for time delay power systems", Energy Conversion and Management, vol. 49, no. 2, pp. 193–204, 2005.
14. A. Khodabakhshian and M. Edrisi, "A new robust PID load frequency controller", Control Eng. Practice, vol. 16, no. 9, pp. 1069–1080, Sept., 2008.
15. W. Tan, "Unified tuning of PID load frequency controller for power systems via IMC", IEEE Trans. Power Syst., vol. 25, no. 1, pp. 341–350, Feb. 2010.
16. W. Zhang, M. S. Branicky and S. M. Phillips, "Stability of networked control systems", IEEE Control Systems, vol. 21, no. 1, pp. 84–99, 2001.
17. C. Edwards, E. F. Colet and L. Fridman, "Advances in variable structure and sliding mode control", Berlin Heidelberg: Springer Verlag, 2006.

18. M. V. Basin and P.C. Rodriguez-Ramirez, "Sliding mode controller design for stochastic polynomial systems with unmeasured states", IEEE Transactions on Industrial Electronics, vol. 61, no. 1, pp. 387–396, 2014.
19. Y. Wang, R. Zhou, and C. Wen, "Robust load-frequency controller design for power systems", Proc. Inst. Elect. Eng. C, vol. 140, no. 1, pp.11–16, Jan. 1993.
20. E. Peter, Kloeden and E. Platen, "Numerical solution of stochastic differential equations", New York, Springer-Verlag Berlin Heidelberg, 1992.
21. L. Wu, Y. Gao, J. Liu, and H. Li, "Event-triggered sliding mode control of stochastic systems via output feedback", Elect. Power Compon. Syst., vol. 33, no. 3, pp. 315–331, April. 2017
22. S. C. Tripathy, R. Balasubramanian and P. S. C. Nair, "Effect of superconducting magnetic energy storage on automatic generation control considering governor dead band and boiler dynamics", IEEE Transition on Power System, vol. 7, no.3, pp. 1266–1273, Aug. 1992.
23. M. T. Angulo, L. Fridman, and A. Levant, "Robust exact finite-time output based control using high-order sliding modes", Intern. J. Syst. Sci., 2011.
24. V. I. Utkin, "SlidingModes in Control Optimization", Berlin, Germany: Springer-Verlag, 1992.
25. J. L. Lee and W. J. Wang, "Robust decentralized stabilization via sliding mode control", Control Theory Adv. Technol., vol. 10, no. 9, pp. 622–631, Sep. 1993.
26. Y. S. Lu and J. S. Chen, "Design of a perturbation estimator using the theory of variable structure systems and its application to magnetic levitation systems", IEEE Trans. Ind. Electron., vol. 42, no. 3, pp. 281–289, June, 1995.
27. K. C. Hsu, "Decentralized variable structure model-following adaptive control of interconnected systems with series nonlinearities", Int. J. Syst. Sci., vol. 29, no. 4, pp. 365–372, Apr. 1998.
28. K. K. Shyu and H. J. Shieh, "A new switching surface sliding mode speed controller for induction motor drive systems", IEEE Trans. Power Electron., vol. 11, no. 4, pp. 660–667, Jul. 1996.
29. R. Khasminskii, "Stochastic stability of differential equations", Springer Science and Business Media. 2011.
30. X. Li, and C.E. de Souza, "Criteria for robust stability and stabilization of uncertain linear systems with state delay", Automatica, vol. 33 no. 9, pp. 1657–1662, 1997.